

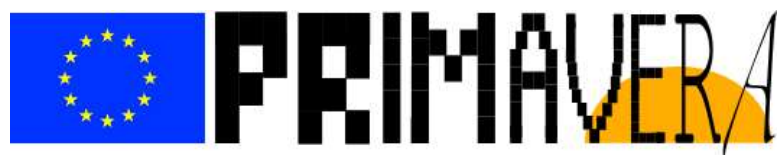


Call: H2020-SC5-2014-two-stage

Topic: SC5-01-2014

PRIMAVERA

Grant Agreement 641727



PRocess-based climate sIMulation: AdVances in high resolution modelling and European climate Risk Assessment

Deliverable D5.2

Report documenting the impacts of AMV and IPV, and changes in direct radiative forcing, on the European climate of the most recent period and sensitivity to resolution and physics choices.

Deliverable Title	Report documenting the impacts of AMV and IPV, and changes in direct radiative forcing, on the European climate of the most recent period and sensitivity to resolution and physics choices.		
Brief Description	The deliverable reports the results of the coordinated multi-model, multi-resolution climate model experiments designed to assess the climate impact of the Atlantic Multidecadal Variability mode, and how these impacts are influenced by model resolution and model physics choices.		
WP number	WP5		
Lead Beneficiary	UREAD		
Contributors	<i>Dan Hodson (UREAD)</i> <i>Paul-Arthur Monerie (UREAD)</i> <i>Yohan Ruprich-Robert (BSC)</i> <i>Emilia Sanchez Gomez (CERFACS)</i> <i>Jorge Lopez Parages (CERFACS)</i> <i>Laurent Terray (CERFACS)</i> <i>Katja Lohman (MPI)</i> <i>Chris Roberts (ECMWF)</i>		
Creation Date	5/2/2020		
Version Number	1.0		
Version Date	5/2/2020		
Deliverable Due Date	31/1/2020		
Actual Delivery Date	5/2/2020		
Nature of the Deliverable	R	<i>R – Report</i> <i>P - Prototype</i> <i>D - Demonstrator</i> <i>O - Other</i>	
Dissemination Level/Audience	PU	<i>PU - Public</i> <i>PP - Restricted to other programme participants, including the Commission services</i> <i>RE - Restricted to a group specified by the consortium, including the Commission services</i> <i>CO - Confidential, only for members of the consortium, including the Commission services</i>	

Version	Date	Modified by	Comments
1.0	5/2/2020	Dan Hodson (UREAD)	Synthesizing and collation contributions from co-authors.

Contents

1.	Executive Summary	4
	<i>Experimental Design</i>	4
	<i>Impacts over Europe</i>	4
	<i>Euro Mediterranean impacts</i>	5
	<i>Pacific Ocean impacts</i>	5
	<i>Impacts on the Global Monsoon system</i>	5
	<i>Conclusions</i>	5
2.	Project Objectives	6
3.	Detailed Report:	7
3.1	<i>Introduction</i>	7
3.2	<i>Modifications to WP5 Experimental plan</i>	9
3.3	<i>Models and Experimental Design</i>	11
	<i>Model descriptions</i>	11
	<i>Experimental Design</i>	13
3.4	<i>Results</i>	15
	3.4.1 <i>Global response of models to AMV forcing</i>	16
	3.4.2 <i>Seasonal Response of European Region to the AMV</i>	17
	3.4.3 <i>The impact of Atlantic Multi-decadal variability on Euro-Mediterranean summer heat waves</i>	28
	3.4.4 <i>Pacific Response to the AMV</i>	34
	3.4.5 <i>Global Monsoon response to AMV</i>	39
3.5.	<i>Conclusions</i>	42
	<i>Assessment for the future</i>	42
3.6.	<i>References</i>	43
3.7.	<i>Peer Review articles</i>	46
3.8.	<i>Planned future Publications</i>	46
4.	Lessons Learnt.....	47
	<i>Scientific</i>	47
	<i>Technical</i>	47
5.	Links Built.....	47

1. Executive Summary

This deliverable summarises the results for the PRIMAVERA WP5 T5.1 experiments. These coordinated multi-model multi-resolution experiments were designed to examine the global climate system's response to key observed multidecadal modes of Sea Surface Temperature (SST) variability. These key modes are the Atlantic Multidecadal Variability (AMV) mode and the Interdecadal Pacific Variability (IPV) mode. This multi-model multi-resolution experiment also allow us to examine how sensitive these modelled impacts are to the specific climate model used and the horizontal grid resolution that model is configured to use.

Experimental Design

We agreed to follow a modified form of the experimental design specified for the Coupled Model Intercomparision Project 6 (CMIP6) DCPP-C subproject. This design provided a simple pre-tested methodology for imposing SST anomalies in coupled climate models and would allow us to begin experiments earlier in the project. It became clear that because of the unexpectedly high computational cost of the new high resolution model configurations, it would not be possible for all five modelling groups to perform both the AMV and the IPV experiment. It was therefore decided that the WP5 partners would only perform the experiments testing the impact of the AMV mode.

Impacts over Europe

We modelled the impacts of the AMV on European climate using five different climate models (**Table 2**) using bother low and high spatial resolution configurations of the model. We concentrate on the impact on three key climate variables: surface air temperature (tas), mean sea-level pressure (psl) and precipitation (pr).

Surface air temperature

The AMV drives a significant warming over western and southern Europe in all seasons (**Figure 4**). The warming in central and northern Europe is much weaker and not statistically significant.

Mean sea level pressure

The AMV drives significant changes in mean sea level pressure over Europe (**Figure 5**). These changes in pressure, and their associated changes in atmospheric circulation, vary across the seasons with western and southern Europe more strongly impacted in Autumn and Winter and northern and eastern Europe more impacted in Spring and summer. These changes in circulation may in part explain the weak warming signal in central Europe (**Figure 4**), as the induced circulations may drive colder air over central Europe, counteracting the direct warming effect.

Precipitation

The AMV drives significant changes in precipitation (**Figure 6**). These changes are mostly confined to north, west and southern Europe and vary notably across the seasons. During Autumn and Winter, the AMV drives increased precipitation over the west coast of Europe. During spring and summer, the AMV drives increased precipitation over the northern most parts of Europe, and a reduction in precipitation over parts of the Euro Mediterranean region.

Impacts of model choice

We repeated the AMV forcing experiments with five different coupled climate models. Using ANOVA, we examined how the AMV impacts described above vary across the models for

each of the three climate variables. We found that the impacts were generally robust to the choice of model. There were two notable exceptions; surface air temperatures north of Scandinavia (**Figure 8**) and mean sea level pressure and surface air temperatures over the Euro Mediterranean region during summer (**Figure 7c, Figure 8c**). The former is likely due to differences in the response of the seasonal sea ice to the AMV between models. The impact over the Euro Mediterranean is discussed below.

Impacts of Resolution

We repeated the AMV forcing experiments at two different resolutions (low and high). We again use ANOVA to test how changing model resolution affects how the AMV impacts climate. Overall, we find that the climatic response to the AMV is generally insensitive to this increase in climate model resolution. One exception is over small regions of high European topography, where increasing resolution does affect how the AMV drives precipitation changes. (**Figure 10**).

Euro Mediterranean impacts

We further examined the impact of the AMV on Euro Mediterranean region in two climate models. Here the AMV drives summertime warming, drying and an increased incidence of heatwave days (**Figure 12-14**). Analysis suggest this arises due to increased subsidence over the region, driven my AMV-induced changes to the West African Monsoon system.

Pacific Ocean impacts

The AMV drives climatic changes outside of the Atlantic Basin. In particular, the AMV drives a widespread cooling in the tropical Pacific Ocean, together with widespread changes in surface air temperature over North America (**Figure 18**). The former is driven by AMV induced changes to the Walker circulation.

Impacts on the Global Monsoon system

The AMV induces widespread impacts on the global monsoon system (**Figure 21**), leading to significant latitudinal shifts, resulting in some regions receiving less monsoon rains, and some regions more.

Conclusions

These experimental results demonstrate that the AMV had a widespread range of impacts on climate over Europe and beyond. These results are generally robust to the choice of model used to perform the experiment, although there are some notable regions where model uncertainties remain. These results are also generally insensitive to the increase in model resolution we have used in these experiments, although there are some changes seen in small regions of high topography.

2. Project Objectives

With this deliverable, the project has contributed to the achievement of the following objectives (DOA, Part B Section 1.1) WP numbers are in brackets:

No.	Objective	Yes	No
A	To develop a new generation of global high-resolution climate models. (3, 4, 6)		X
B	To develop new strategies and tools for evaluating global high-resolution climate models at a process level, and for quantifying the uncertainties in the predictions of regional climate. (1, 2, 5, 9, 10)	✓	
C	To provide new high-resolution protocols and flagship simulations for the World Climate Research Programme (WCRP)'s Coupled Model Intercomparison Project (CMIP6) project, to inform the Intergovernmental Panel on Climate Change (IPCC) assessments and in support of emerging Climate Services. (4, 6, 9)		X
D	To explore the scientific and technological frontiers of capability in global climate modelling to provide guidance for the development of future generations of prediction systems, global climate and Earth System models (informing post-CMIP6 and beyond). (3, 4)		X
E	To advance understanding of past and future, natural and anthropogenic, drivers of variability and changes in European climate, including high impact events, by exploiting new capabilities in high-resolution global climate modelling. (1, 2, 5)	✓	
F	To produce new, more robust and trustworthy projections of European climate for the next few decades based on improved global models and advances in process understanding. (2, 3, 5, 6, 10)	✓	
G	To engage with targeted end-user groups in key European economic sectors to strengthen their competitiveness, growth, resilience and ability by exploiting new scientific progress. (10, 11)		X
H	To establish cooperation between science and policy actions at European and international level, to support the development of effective climate change policies, optimize public decision making and increase capability to manage climate risks. (5, 8, 10)	✓	

3. Detailed Report:

This report details the research conducted within T5.1 in Work Package 5 (WP5) within PRIMAVERA. The aim of WP5 is to improve our understanding of the influence of a selected range of European climate drivers at decadal time scale as well as the associated mechanisms and their robustness to climate model resolution and physics.

This report section is set out as follows. **Section 1** Introduces decadal climate variability. **Section 2** details the modifications to the WP5 experimental plan. **Section 3** outlines the Models and methodology used in the experiments in WP5. **Section 4** presents the results of the analysis of these experiments. **Section 5** then discusses these results and presents our conclusions.

3.1 Introduction

The aim of T5.1 is to examine the AMV and IPV modes and their impact on European climate.

During the last century, the global oceans have exhibited slow, multidecadal fluctuations in Sea Surface Temperatures (SST). The two leading modes of decadal climate variability across the globe are the Atlantic Multidecadal Variability (AMV - **Figure 1, Kerr 2000**) mode and the Interdecadal Pacific Variability (IPV - **Figure 2, Henley 2015**) mode. The underlying driver of these modes of variability is an area of active research.

The IPV is thought to drive far-reaching climate impacts over Australia, the US and further afield (**Dong 2015**), and is comparable to a decadal modulation of ENSO teleconnections.

The AMV is thought to be at the origin of marked climate anomalies with substantial impacts upon human activities over many areas of the globe. Previous studies proposed a causal link between the warm phase of the AMV and warm conditions over Central Europe, dry conditions over the Mediterranean basin, and wet conditions over Northern Europe (**Sutton 2012**), modulating the river streamflow (**Enfield 2001**), electricity production (**Kirchner-Bossi 2015**), droughts over Africa (in particular the extremely severe 70s-80s Sahelian drought (**Zhang 2006**)) and North America (**McCabe 2004**), and changes in tropical cyclone activity (**Zhang 2006**). The AMV may also impact the location and activity of the North Atlantic extratropical storms by modulating the large-scale atmospheric circulation. Given the numerous potential

climate impacts of the AMV and their related consequences on human society, a greater understanding of these teleconnections and their predictability has the potential to deliver significant societal benefits

Studies examining observations and climate model experiments suggest that the AMV may arise as a response to slow changes in the deep ocean circulation (AMOC) (**Knight 2005**), or anthropogenic sulphate aerosol emissions (**Booth 2012**), or even changes in solar variations or volcanoes (**Otterå 2010**). Whatever the ultimate drivers of the AMV and IPV, such large-scale changes in Sea Surface Temperatures (SSTs) are likely to themselves drive significant changes in climate, as discussed above. If we can further understand the role these decadal modes play in driving decadal variations in climate, we may be able to improve forecasts of future decadal variations in climate.

To robustly elucidate the impacts of the AMV we need to turn from observational studies to experiments with climate models. Studies of the impacts of the AMV with simpler atmosphere-only models driven by Sea Surface Temperatures (SSTs) have demonstrated that the observed changes in AMV had a significant impact on land surface temperature, precipitation and surface atmospheric circulation (**Sutton and Hodson 2005**).

Simple experiments like this using Atmosphere-only models driven by a fixed SST boundary condition suffer from the inability of the ocean to respond to any forced changes in climate. This feedback between the ocean and atmosphere may then result in an equilibrium climate response that differs from the simpler direct atmosphere-only response. A number of studies have addressed this issue by performing a modified form of these experiments using an Atmosphere-Ocean coupled climate model (e.g. **Ruprich-Robert 2017**).

Such experiments have been conducted with only a few different climate models, so the question naturally arises as to how robust these results are across a range of climate models?

DCPP-C is a subproject within CMIP6 (Coupled Model Intercomparison Project 6) designed to examine this issue. It adopts a modified form of the experimental protocol used by **Ruprich-Robert (2017)** and specifies a uniform methodology that can be applied across a wide range of Atmosphere-Ocean coupled climate models.

This methodology, whilst addressing the question of model dependence on the results, does not explicitly address the question of a dependence of the results on *model resolution* - that is the fidelity (i.e. number of gridpoints) with which each climate model represents the atmosphere and ocean. There are good reasons to believe that the climate response may be different at a higher resolution, as additional responses may be captured that are not resolved at a lower resolution.

T5.1 within WP5 has been explicitly designed to address this issue. We have performed the DCPP-C AMV experiments using a set of climate models at standard model resolution, and then repeated these experiments at a finer model resolution. Examining any differences between the responses between these two sets of experiments will show where increased model resolution adds extra value. This is important, as increasing model resolution leads to increased computational costs; it is therefore important to know whether such increased costs are worthwhile in forecasting terms.

3.2 Modifications to WP5 Experimental plan

The initial WP5 plan was to perform both AMV and IPV experiments, as specified under the DCPP-C protocol, using both contemporary and future radiative forcings. However, when the computational costs of running the experiments with the new generation of coupled climate models at the higher resolution were evaluated, it was found that the existing computational resources would not allow both the AMV and IPV experiments to be performed by all groups. It was therefore decided that WP5 would concentrate on the AMV experiments only, using contemporary radiative forcings only. It also became apparent that the full AMV experiment as specified in DCPP-C was also too costly to perform at the high resolution. We therefore decided to slightly modify the DCPP-C design to allow the experiments to be performed with the computational resources available. Full details of these modifications are presented in **Section 3**

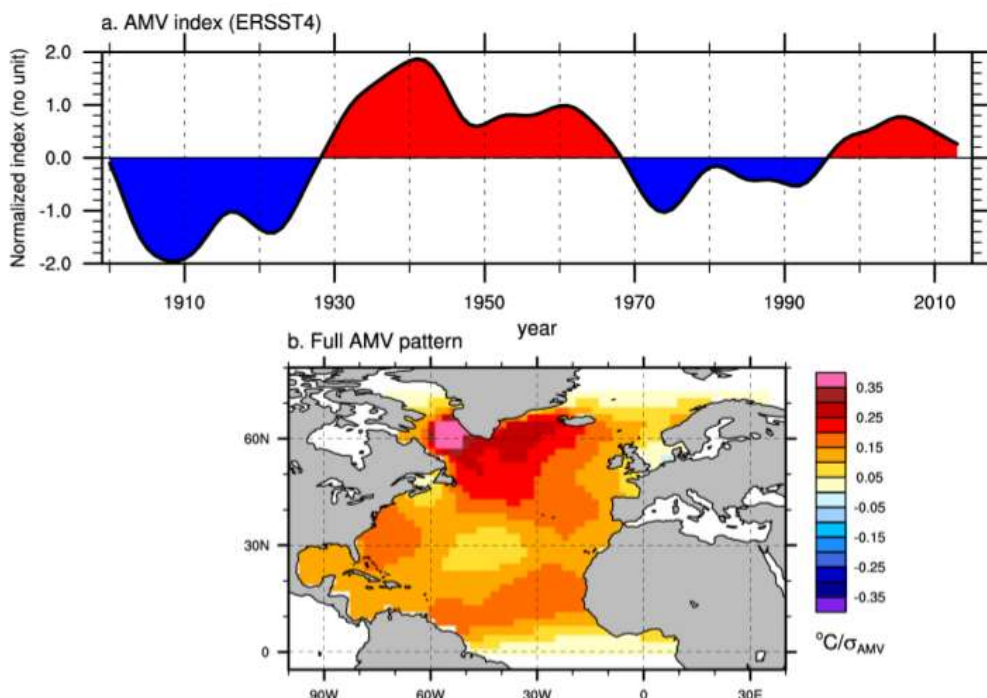


Figure 1: a) AMV index computed from ERSST4 Sea Surface Temperatures (0:60N, 7.5W:75W). The index has been detrended and smoothed using a 10-year Butterworth filter. b) AMV SST anomaly obtained from regression of ERSSTv4 annual residual SST (i.e. forced component removed) on the AMV time-series (a). Contour Interval is 0.05 C/ σ . Reproduced from Technical Note for DCPP-C <http://www.wcrp-climate.org/wgsip/documents/Tech-Note-1.pdf>

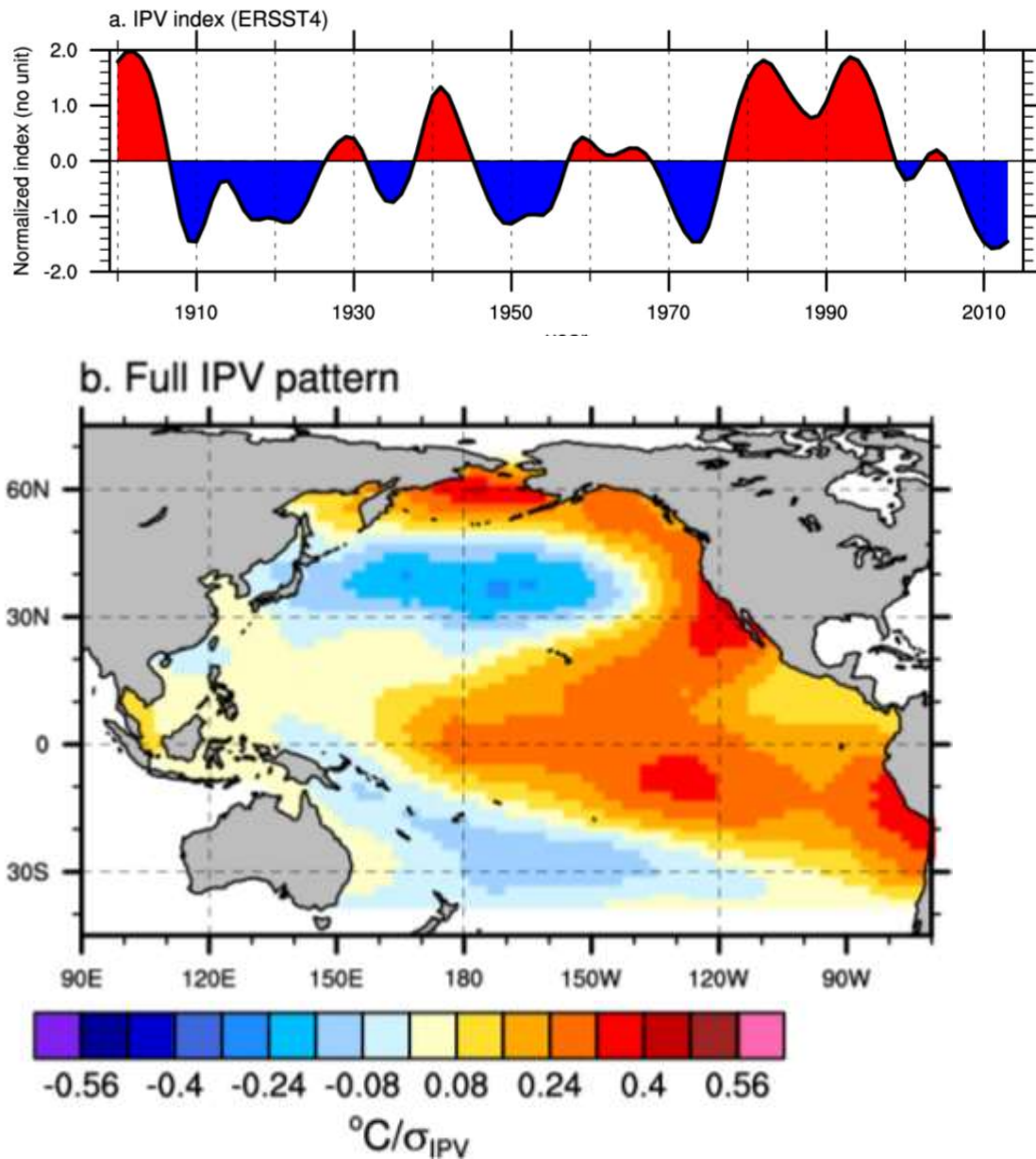


Figure 2: a) Normalized IPC time series (2nd EOF 40S:60N) after filtering (13 year Butterworth). b) IPC SST anomalies obtained from regression of ERSSTv4 annual residual SST (i.e. forced component removed) on to the IPV time series, Contour interval is 0.08 C/ σ . Reproduced from Technical Note for DCPP-C - see <http://www.wcrp-climate.org/wgsip/documents/Tech-Note-1.pdf>

3.3 Models and Experimental Design

The WP5 partners performed the AMV experiments with five different coupled climate models. These were:

Model	Partners
CNRM-CM6-1	CERFACS
EC-Earth	BCS/CNR
ECMWF-IFS	ECMWF
MetUM-GOML2	Reading/NCAS
MPIESM1.2	MPI

Model descriptions

Brief descriptions of these climate models and their formulations are given below:

CNRM-CM6-1

CNRM-CM6-1 is coupled climate model consisting of the ARPEGE-Climat (**Déqué et al., 1994**) atmospheric model coupled to the NEMO v3.6 ocean model (**Madec et al., 2017**) via the OASIS3-MCT coupler (**Craig et al., 2017**). The model also includes a land surface scheme (ISBA - **Noilhan & Planton, 1989**), the GELATO v6 (**Salas Méria, 2002**) sea ice model , the SURFEX (**Masson et al., 2013**) externalized surface interface model , and the CTRIP (**Decharme et al., 2019**) river routing scheme .For full details see (**Volodire 2019**).

The Atmosphere is a spectral model with 91 vertical levels and a horizontal truncation of T127, resulting in a resolution at the equator of about 1.4°. The ocean has 75 vertical levels and a horizontal resolution of about 1°, reducing to 1/3° in the tropics.

EC-Earth

The EC-Earth3P and EC-Earth3P-HR models are fully detailed in **Haarsma et al.**

(2020). Their atmospheric component is based on the cycle 36r4 of the Integrated Forecast System (IFS) atmosphere-land-wave model of the European Centre for Medium Range Weather Forecasts (ECMWF). It uses a reduced Gaussian-grid with 91 vertical levels and a T255 horizontal truncation / N128 grid resolution (~100 km) for EC-Earth3P and a T511 horizontal truncation / N256 grid resolution (~50km) for EC-Earth3P-HR. The H-TESSEL model is used for the land surface (**Balsamo et al., 2009**) and is an integral part of IFS: for more details see **Hazeleger et al. (2012)**. The ocean component comes from the version 3.6 of the Nucleus for European Modelling of the Ocean (NEMO; **Madec 2017**). Both configurations share a 75 vertical levels resolution but differ on their nominal horizontal resolution of 1° for EC-Earth3P (with meridional refinement down to 1/3° in the tropics) and 0.25° for EC-Earth3P. The ice model, embedded in NEMO, is the Louvain la Neuve sea-ice model version 3 (LIM3, **Vancopenolle et al. 2012**), which is a dynamic-thermodynamic sea-ice model with 5 thickness categories. The atmosphere and ocean/sea ice parts are coupled through the OASIS (Ocean, Atmosphere, Sea Ice, Soil) coupler (**Valcke 2013**).

ECMWF-IFS

ECMWF-IFS is a global Earth system model that includes dynamic representations of the atmosphere, sea-ice, ocean, land surface, and ocean waves. A detailed description of the ECMWF-IFS-HR and ECMWF-IFS-LR configurations used in this study, including scientific assessment of the coupled model performance, is provided in **Roberts et al. (2018)**. ECMWF-IFS is based on the IFS atmosphere-land-wave model (cycle 43r1) coupled to version 3.4 of the Nucleus for European Models of the Ocean (NEMO) (**Madec 2017**) and version 2 of the Louvain-la-Neuve Sea-Ice Model (LIM2; **Bouillon et al. 2009; Fichefet and Maqueda 1997**). ECMWF-IFS-HR uses the Tco399 grid (~25 km) in the atmosphere and NEMO ORCA025 grid (~25 km) for ocean-sea-ice. ECMWF-IFS-LR uses the Tco199 grid (~50 km) in the atmosphere and NEMO ORCA1 grid (~100 km) for ocean-sea-ice. One of the significant differences between these configurations is the use of the **Gent and Mcwilliams (1990)** parameterization for the effect of mesoscale eddies with the ORCA1 grid, which is disabled when using the ORCA025 grid. Both ocean configurations use the same vertical discretization, which consists of 75 z-levels and partial cells at the ocean floor.

MetUM-GOML2

MetUM-GOML2 is an ocean mixed-layer coupled configuration of the Met Office Unified Model (MetUM-GOML2; **Hirons et al. 2015**); combining the atmosphere component from HadGEM3 (GA6.0; **Walters et al., 2017**) coupled to a Multi-Column K Profile (MC-KPP) mixed layer Ocean model (**Hirons et al., 2015**) via the Ocean Atmosphere Sea Ice Soil (OASIS) coupler (**Valcke, 2013**). For full details of MetUM-GOML2 see (**Hirons et al. 2015**) The atmosphere and ocean have a horizontal resolution of either 1.25 x 1.87° (~200km, N96 - LR) or 0.833 x 0.55° (~100km, N216

- HR). The Atmosphere has 85 vertical levels whilst the ocean mixed-layer component extends to 1km depth with 100 vertical levels. Sea ice fraction is prescribed from 1976-2005 mean climatology, as is Sea Surface Temperature in regions that are not ice-free all year.

Although there is vertical ocean mixing, there is no horizontal advection or mixing in the model; these terms are replaced by seasonally-varying 3d temperature and salinity flux corrections, diagnosed from seasonal climatologies. Consequently, MetUM-GOML2 has small sea surface temperature biases and small model drifts (**Hirons et al., 2015**). We use a 1976-2005 mean ocean temperature and salinity reference climatology, derived from the Met Office ocean analysis (**Smith & Murphy, 2007**). Anthropogenic greenhouse gases concentration, aerosol emissions, volcanic activity imposed and kept constant to their mean value of the period 1976-2005.

MPIESM1.2

MPI-ESM (version 1.2.01), consisting of the atmosphere component ECHAM6.3 (**Stevens et al. 2013**) including the land-surface scheme JSBACH, the combined ocean and sea ice component MPIOM1.6.3 (**Jungclaus et al. 2013**) including the ocean biogeochemical component HAMOCC. Ocean and atmosphere are coupled through the OASIS3 coupler (**Valcke et al. 2013**) with a coupling frequency of one hour. The atmosphere component applies a spectral grid at truncation T127 (about 1-degree, low-resolution version) or T255 (about 0.5 degree, high-resolution version) and 95 hybrid levels. The ocean component applies a tripolar grid (two northern poles) with a nominal resolution of 0.4 degree and 40 unevenly spaced z-levels. The first 20 levels are distributed over the upper 700 metres of the water column. A partial grid cell formulation is used to better represent the bottom topography.

Experimental Design

We follow a modified form of the DCPP-C AMV experimental design. Full details of this design are given in (**Boer 2016**). We now briefly outline this experimental design and the modifications we have used in the WP5 AMV experiments.

DCPP-C

The goal of the DCPP-C AMV experiments is to force the global coupled atmosphere-ocean climate system with an AMV spatial SST pattern that represents the observed spatial pattern of AMV variability. This forcing needs to be achieved without restricting the ocean's ability to respond to any atmospheric changes the AMV forcing might drive.

The AMV pattern (**Figure 1**) used in the experiments is derived from an observed SST product (ERSSTv4, **Huang et al 2016**)

Externally Forced Signal

First an estimate of the externally forced SST trend is removed from the SST at every gridpoint. This externally forced SST trend is estimated using the CMIP5 historical (and RCP8.5) multimodel ensemble. A signal-to-noise maximizing EOF analysis is used to extract the leading mode of common variability. The timeseries (PC) associated with this leading mode is an estimate of the externally forced response - due to greenhouse gases, aerosol, solar and volcanic variations.

AMV Pattern

This estimate of the externally forced response is then removed from every SST gridpoint by regression. An AMV index is then computed from the resulting detrended SST dataset by averaging over 0:60N within the Atlantic region (**Figure 1a**). The resulting timeseries is then smoothed using a 10-year filter to retain only multidecadal variations. The final AMV spatial pattern (**Figure 1b**) is produced by regressing the detrended SST dataset onto this smoothed AMV index.

Forcing Methodology

The AMV SST pattern is then used to drive a coupled climate model as follows.

First a Preindustrial SST climatology is computed from a pre-existing Preindustrial control run for a model. The AMV pattern is added (subtracted) from this climatology to produce an AMV+ (AMV-) target SST field. The model is then initialised Preindustrial control conditions. Model SSTs within the North Atlantic (SST_{model} : AMV region, using a predefined mask) are then nudged towards the target SST field ($SST_{target} = \text{Climatology} +/- \text{AMV}$) using an additional surface heat flux term ($hfcorr$) of the form:

$$hfcorr = -40 (SST_{model} - SST_{target})$$

The prefactor of -40 W/m²/K was chosen based on a range of sensitivity studies used to design the DCPP-C experiments. For more details see <http://www.wcrp-climate.org/wgsip/documents/Tech-Note-2.pdf>

An ensemble of integrations of the model is then performed, all starting from different atmosphere and ocean initial conditions taken from the preindustrial control. Each integration is run for a maximum of 10 years, to prevent large drifts building in the ocean which could overwhelm the AMV forced signal. The resulting difference between the AMV+ and AMV- experiments can then be used to assess the climatic impacts of AMV variations.

Modifications for PRIMAVERA WP5

WP5 considered the adoption of the DCPP-C AMV experimental design for WP5 T5.1 to be exceptionally valuable - whilst the design of DCPP-C was not available during the PRIMAVERA proposal period, it was an ideal design to meet WP5 T5.1 goals. It had the additional value that, using a CMIP6 protocol would mean that the resulting

experiments would be of great additional interest to the wider climate science community outside PRIMAVERA.

Adoption of DCPP-C presented some challenges, however, the experimental design was tuned for standard/low resolution climate models, and required a very large number of years of integration (~500), none of the WP5 project partners had the computing resources to integrate their more resource intensive high resolution models for this number of years. For this reason, the WP5 partners decided that each partner would run their high resolution model for ~100 years. However, it was likely that the signal of the climate response to the AMV would be too weak to detect with only 100 years of data using the standard protocol. Therefore, WP5 decided to modify the experimental design by forcing the models with a 2*AMV pattern, to boost the forced signal and hence reduce the number of years required to detect a response.

Additionally, the DCPP-C design calls for a preindustrial control to be integrated to generate the background climatology for the experiment. At the time no institutions had completed their preindustrial control integrations for CMIP6 - and none were considering completing preindustrial controls for their high resolution climate models. However, PRIMAVERA WP6 were integrating a control for 1950s climate forcings, for both the high and low resolution models. For this reason, it was decided to use these 1950s controls, rather than the prescribed preindustrial controls. (For operational reasons MetUM-GOML2 used an observed 1976-2005 mean ocean climatology as the background climatology).

3.4 Results

We now turn to the result of the modified DCPP-C AMV experiments. **Table 2** presents the number of years of experimental data available for each experiment, model and resolution. In **Section 4.1** we overview the mean model surface temperature response to the AMV.

In **Section 4.2** we discuss the overall seasonal mean responses over the European Region. We then examine the impact of resolution and model choice on these results. In **Section 4.3**, we examine the detailed impact of the AMV over the Mediterranean region. In **Sections 4.4 & 4.5** we consider the wider impact of the AMV, in particular the impact on the Pacific, and the Global monsoon system.

Model	Number of ensemble members	
	Low Resolution (~1°)	High Resolution (~0.5°)
CNRM-CM6-1	150	*
EC-Earth	250	70
ECMWF-IFS	300	150
MetUM-GOML2	150	150
MPIESM1.2	100	100

Table 2: AMV experiments - number of ensemble members for the 2AMV+ (2AMV-) experiment for each model and resolution. * Due to technical problems with the high resolution development, it was not possible to conduct the high resolution experiments with CNRM-CM6-1

3.4.1 Global response of models to AMV forcing

We begin by examining the modelled global response of surface air temperature to the AMV forcing pattern. Figure 3 shows that the AMV forcing pattern over the Atlantic (Figure 1b) is well reproduced across the models, and this pattern of forcing persists throughout the year. Figure 3 shows that there are both notable European and wider, global scale impacts. We will discuss the global impacts in sections 3.3-5, but first, in section 3.2, we focus on the direct European impacts of the AMV.

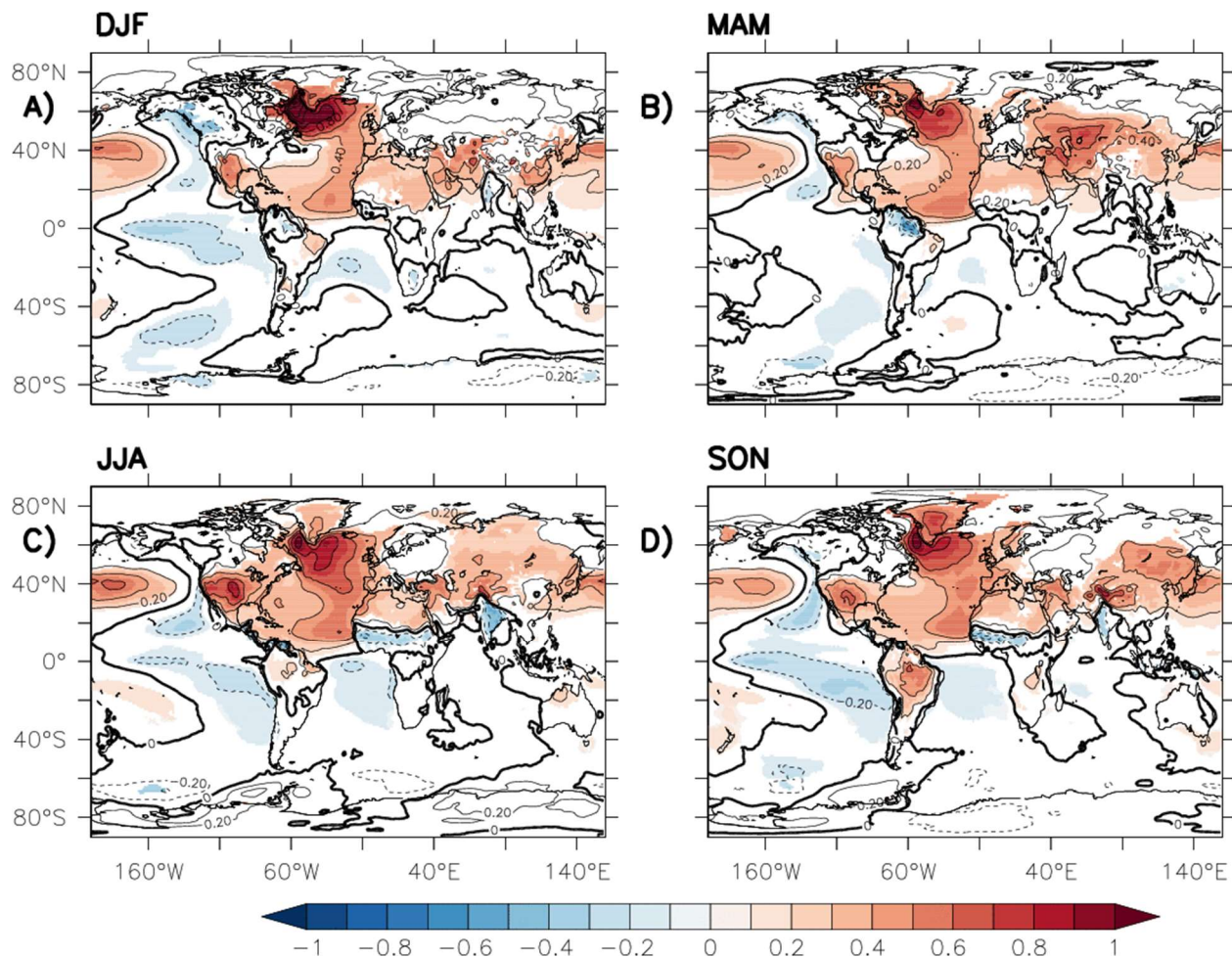


Figure 3: Global seasonal mean surface air temperature (TAS) response ($2^*\text{AMV}^+ - 2^*\text{AMV}^-$) averaged across all five models (Table 2) in their low resolution configuration. Units: C. Shaded areas show regions of statistically significant differences (t-test: $p < 0.05$).

3.4.2 Seasonal Response of European Region to the AMV

We begin by examining the seasonal mean impact of the AMV over the European region across all models at low resolution. We will focus on three key atmosphere variables, surface air temperature (tas), mean sea level pressure (psl) and precipitation (ppt).

In each case, we examine the modelled response to $2^*\text{AMV}^+ - 2^*\text{AMV}^-$. Hence the results show the atmospheric response during periods when the AMV is in the AMV⁺ phase. Assuming linearity in the response, the atmospheric response during periods when the AMV is in the AMV⁻ phase is the negative of all responses shown here.

Surface Air Temperature

Figure 4 shows the seasonal mean surface air temperature (tas) AMV response averaged across all five models (Table 2) in their low resolution configuration. Each season shows a significant warming across the region during the AMV+ phase (and hence a cooling in the AMV- phase). The warming is more pronounced in western and southern Europe (0.2-0.4 C), with a much weaker warming in central, eastern Europe. This pattern of warming is consistent with those found in an earlier study by Ruprich-Robert (2017).

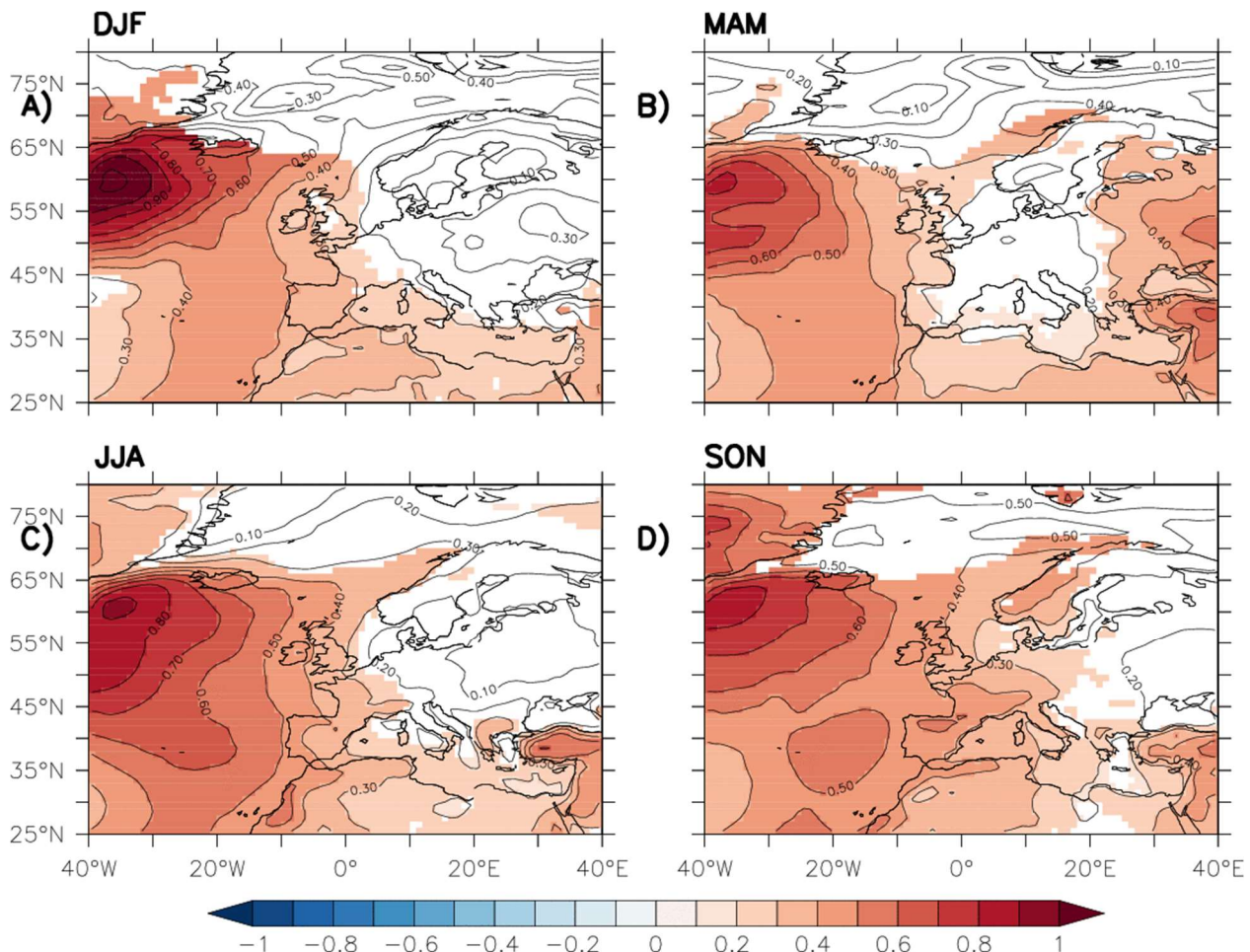


Figure 4: European seasonal mean surface air temperature (TAS) response ($2^*AMV^+ - 2^*AMV^-$) averaged across all five models in their low resolution configuration. Units: C.

Mean Sea Level Pressure

Figure 5 shows the seasonal mean sea level pressure (psl) AMV response averaged across all five models in their low resolution configuration. Each season shows significant changes in atmospheric circulation over the European region. In winter (DJF: **Figure 5a**), a pronounced low pressure anomaly is present west of Europe. This anomalous circulation could drive anomalous advection of heat northwards from the Iberian Peninsula during AMV+ periods; warming wintertime conditions over France, Germany, the UK and Ireland, and conversely driving a cooling during AMV- periods. During spring (MAM: **Figure 5b**), the AMV drives a low pressure anomaly over northern Europe, centred on Finland. The northerly winds associated with this low pressure system may advect colder northern air southwards into central Europe and be responsible for the weaker temperature anomalies seen in spring (**Figure 4b**). Summer (**Figure 5c**), shows significant circulation anomalies across the whole region, with a pronounced low pressure over northern Europe and weaker anomalies over the European-Mediterranean region. In Autumn (**Figure 5d**), the pressure anomalies are generally weaker and confined to southern Europe.

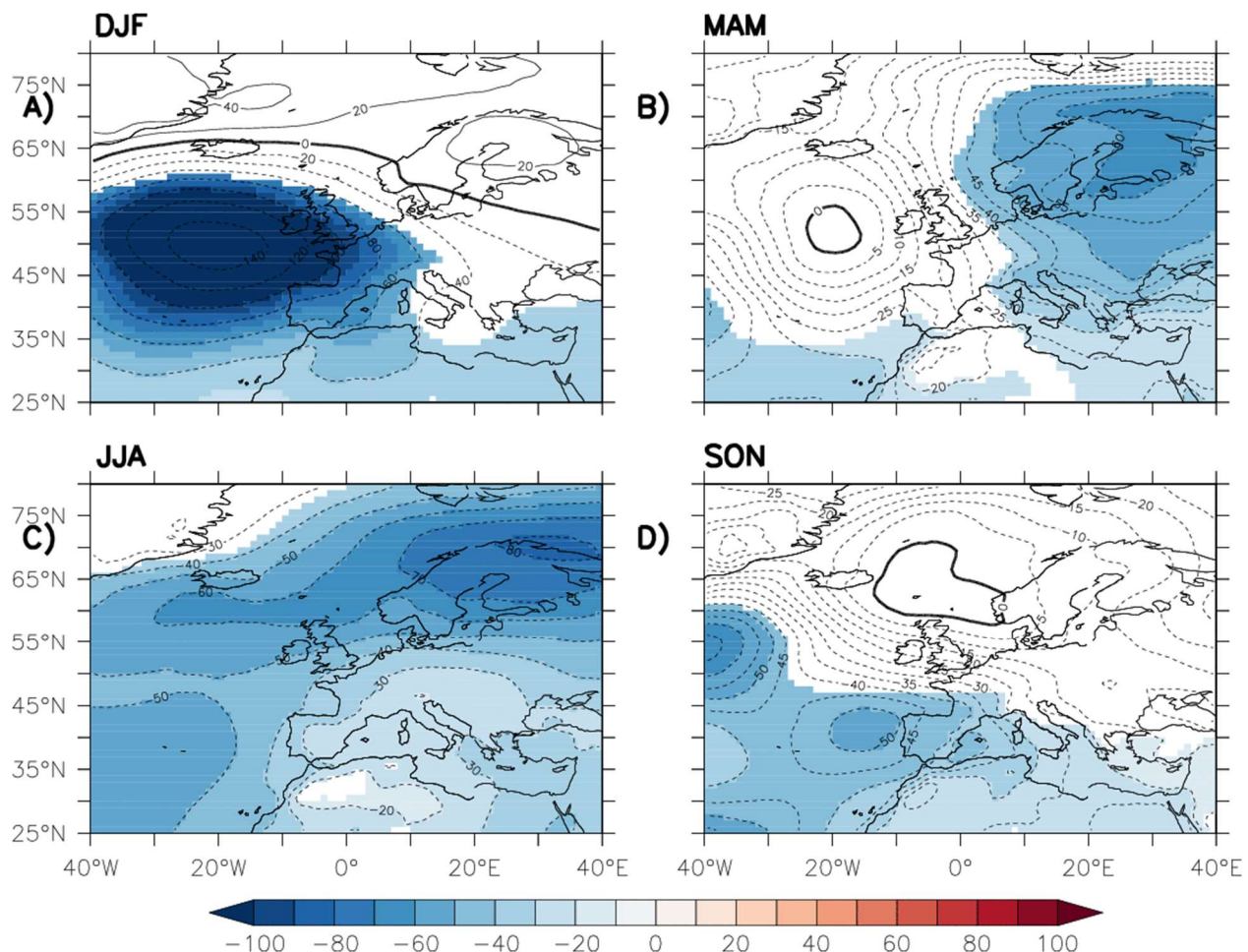


Figure 5: As Figure 4, but for mean sea level pressure (psl). Units: Pa

Precipitation

Figure 6 shows the seasonal precipitation (ppt) AMV response averaged across all five models in their low resolution configuration. Each season shows significant changes in precipitation. Winter (**Figure 6a**) sees increases in precipitation over the western coastal regions of Europe in the AMV+ phase, together with some smaller increases over northern Mediterranean coastal regions. These anomalies may be the result of a southward shift in the storm track associated with the Winter circulation anomaly (**Figure 4a**). Spring (**Figure 6b**), sees small increases in precipitation over central Europe and the northern coast of Norway.

During summer (**Figure 6c**), precipitation increases over northern Europe together with decrease over the Mediterranean region. This latter decrease over the Mediterranean is discussed in more detail in **Section 3.3**. In Autumn (**Figure 6d**) this drying signal appears to move further north over western and central Europe, pushing the increased precipitation signal to the northernmost parts of Europe.

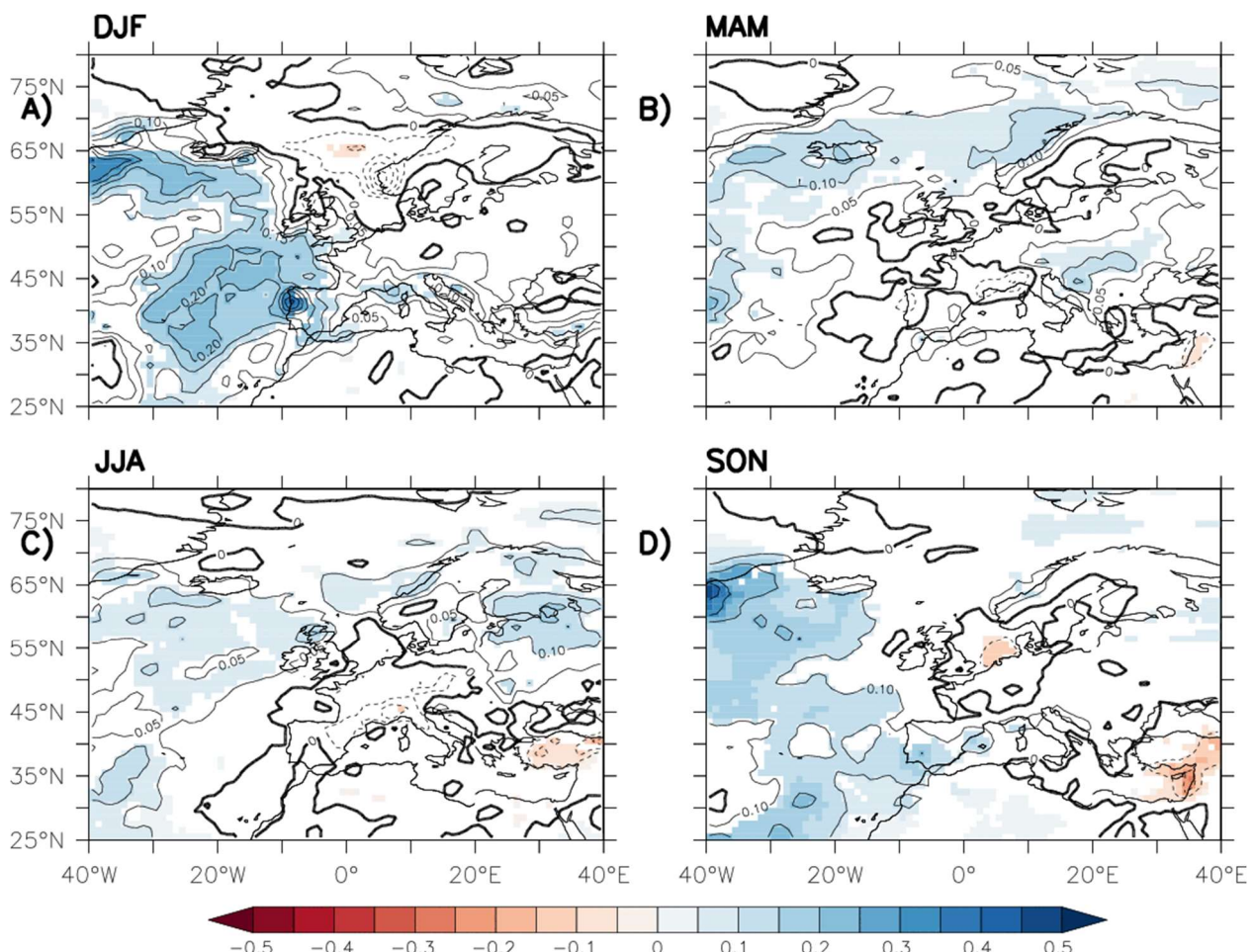


Figure 6: As Figure 4, precipitation (ppt). Units: mm/day

The Impact of model physics

The previous section examined the mean response to the AMV across all five LR models in **Table 2**. We now examine how sensitive these results are to the choice of model, and hence the underlying model physics choices each model represents.

We assess this as follows. We can denote each experiment ensemble member by X_{emj} , where e is the experiment (AMV + or -), m the model (**Table 2**) and j is the ensemble member. Since some models have fewer ensemble members than others, we will only use the 100 ensemble members from each model. For models that have more ensemble members than this, we will randomly subsample the full ensemble.

We can then apply two-way Analysis of Variance (ANOVA), using a model:

$$X_{emj} = M + A_e + B_m + C_{em} + E_{emj}$$

Hence, the variance of full ensemble can be explained by **M** - the mean over all indices, **A** - the AMV phase (+ or -) (as seen in the previous section), **B** - model choice, **C** - the interaction between AMV phase and model choice, and **E** - a noise residual. Standard ANOVA tests can then be used to test the size and significance of each contribution.

A is simply the AMV impact as seen in the previous section. **B**, since it averages across AMV phases, is a measure of the spread in the model climatologies. **C** characterises the influence of model choice on the experimental impact of the AMV (hence the interaction term).

Figure 7 shows **C** for mean sea-level pressure (psl) the impact of model choice on the psl response to the AMV. Here we show **F**, the fraction of variance in **A** explained by **C** for each gridpoint across the region. Where **F** is large, there will be significant disagreement between models about the nature of the response to the AMV. Where **F** is small (or not significant), models agree on the nature of the response to the AMV.

F for mean sea-level pressure is shown in **Figure 7c**. This shows that there is considerable disagreement on the magnitude of the summer (JJA) psl response to the AMV across the models (**Figure 3c**) over central and southern Europe. A similar disagreement is seen in Autumn (**Figure 7d**), but this is confined to the Iberian Peninsula. In Winter and Spring, there are no significant disagreements between the models (not shown) on the mean sea-level pressure response to the AMV, suggesting we can have confidence in the modelled results in these seasons.

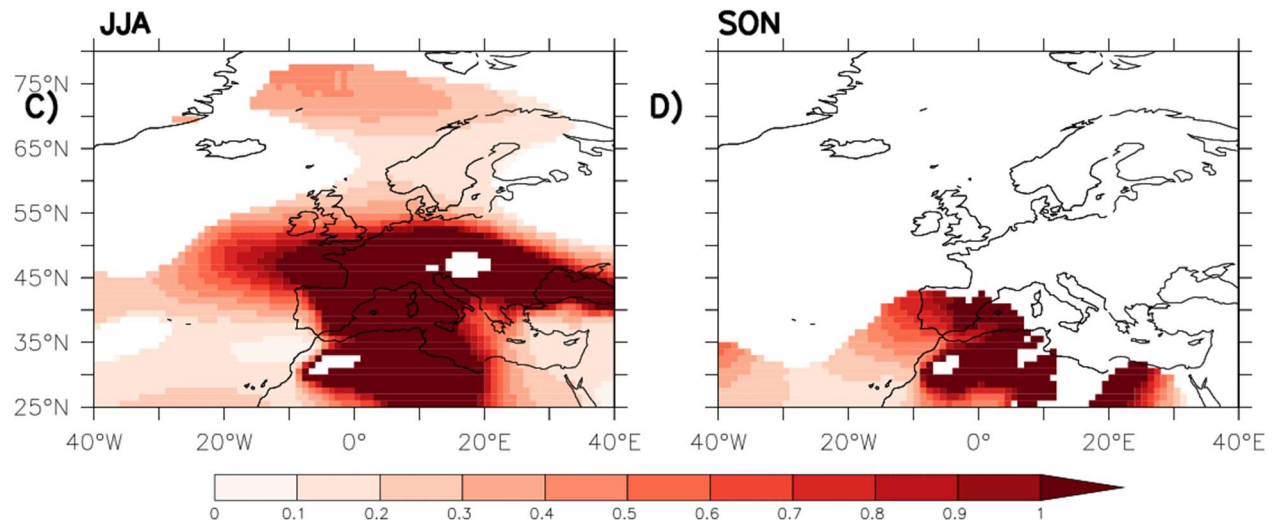


Figure 7: Impact of model choice on the AMV response of mean sea level pressure (PSL: $2^*AMV^+ - 2^*AMV^-$). Fraction of the experiment variance due to model choice.

For surface air temperature (**Figure 8**), the models show more agreement as to the nature of the AMV response. There are disagreements over the ocean, particularly regions north of Scandinavia, peaking in winter (differences in the response of sea-ice to the AMV may be a factor).

There are also small disagreements over the European continent throughout the year, but, in general the models agree on the large-scale surface air temperature response to the AMV.

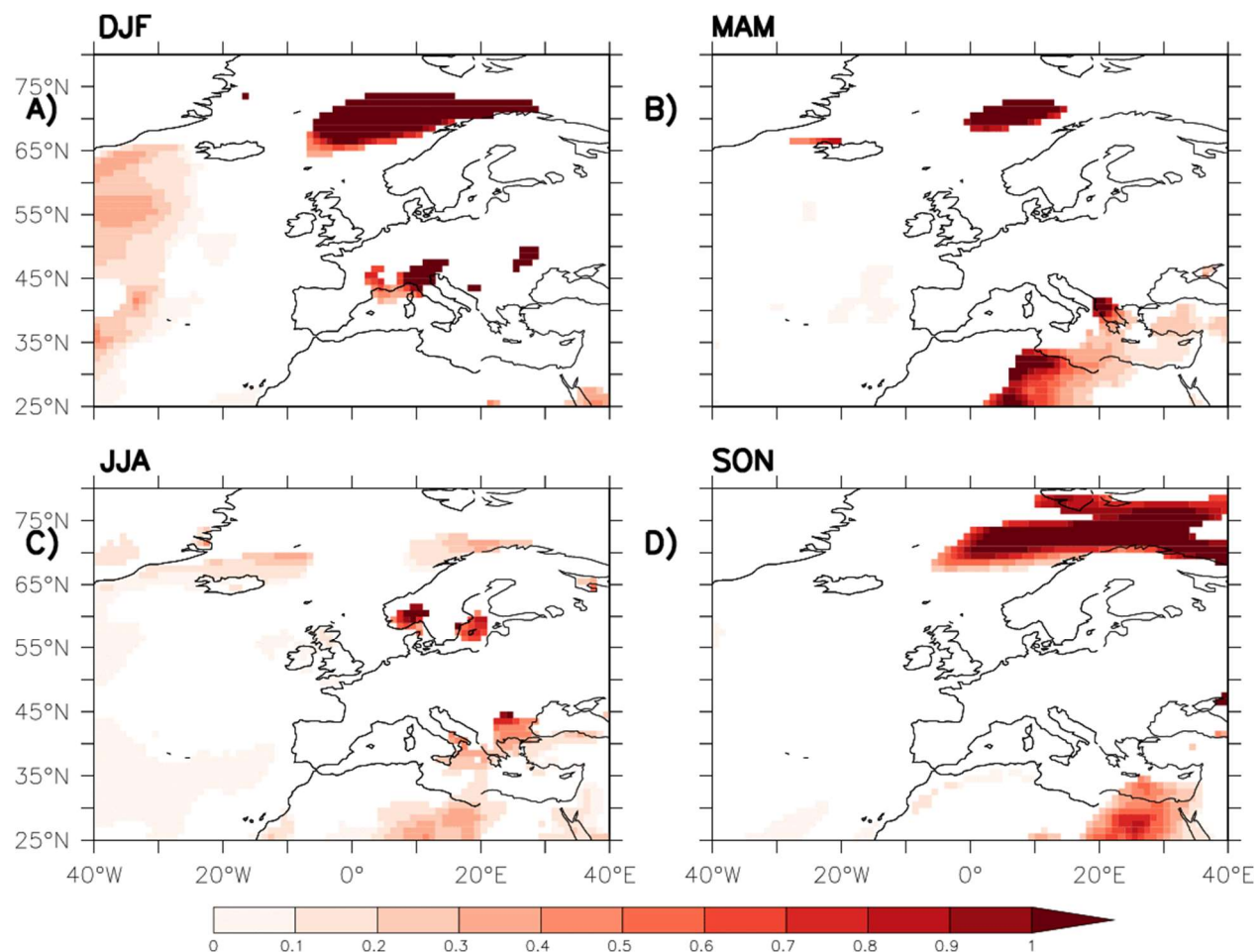


Figure 8: As Figure 7, but for surface air temperature (TAS).

A similar picture emerges for precipitation (pr) across the year (**Figure 9**); there are significant regions where the models disagree on the precipitation response to the AMV, but these are small, and generally confined to regions over the ocean. Where disagreement over land does occur, it does not generally alter the large-scale response seen in **Figure 6**. (One exception may be the response over Scandinavia in summer (JJA **Figure 9c**), where there is disagreement over the response over northern Norway and the Baltic sea region.)

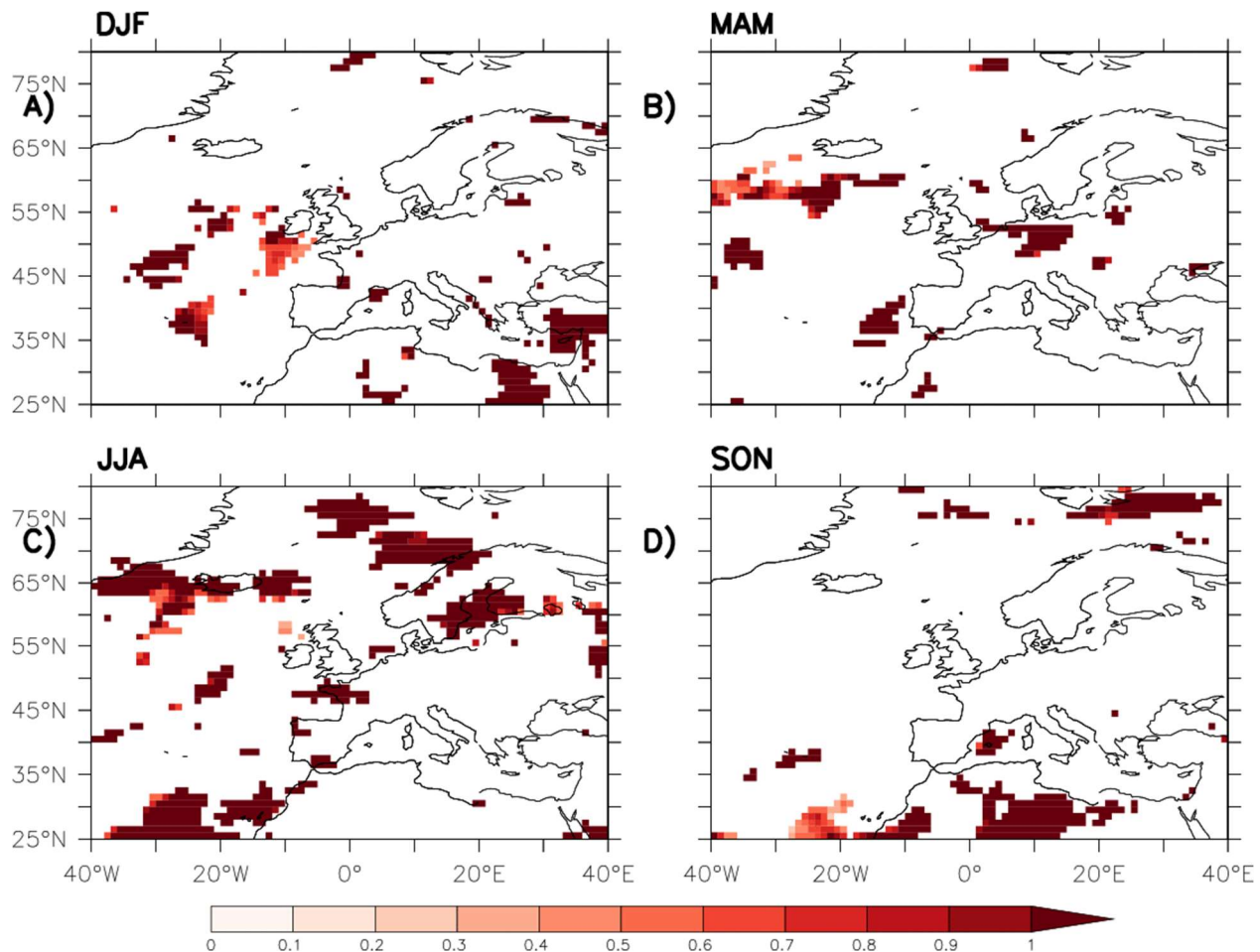


Figure 9: As Figure 7, but for precipitation (PR).

The Impact of model resolution

Finally, we examine the impact that model resolution has on the modelled response to the AMV.

We assess this in a similar manner to above. We now include the high resolution model results (**Table 2**). In order to compare the results by gridpoint, we regrid the high resolution model data to the low resolution grid. Inevitably, detailed spatial information is lost in this process. However, here we are principally concerned with systematic large-scale changes in the modelled response that changes in resolution may cause.

We can again denote each experiment ensemble member by X_{erj} , where e is the experiment, and this time r is the **resolution** (L or H) and j is again the ensemble member. Here we combine all models together to produce a super-ensemble. Since some models have fewer ensemble members at high resolution than low resolution, we will (randomly) select the same number of ensemble members at low and high

resolutions for each model. This results in an ensemble size of ~400 for each resolution (L, H) and AMV phase (+,-) combination.

We then again apply two-way Analysis of Variance (ANOVA), using a model:

$$X_{erj} = M + A_e + B_r + C_{erj} + E_{erj}$$

Since resolution has two distinct categories, we can express the impact of resolution on the AMV response as a quadrature: $(X(H,+)-X(H,-))-(X(L,+)-X(L,-))$

That is, the difference between the AMV response at high resolution, and the AMV response at low resolution. The ANOVA test for **C** allows us to plot the significance of this quadrature.

The results for precipitation (pr) (**Figure 10**) show that there are some significant changes in the modelled response to the AMV as model resolution changes, but these are small and sparse over land. Where small differences exist over land, they tend to be located over regions of high topography (notably in MAM and JJA). Such differences may occur due to the improved resolution of continental topography in the high resolution models.

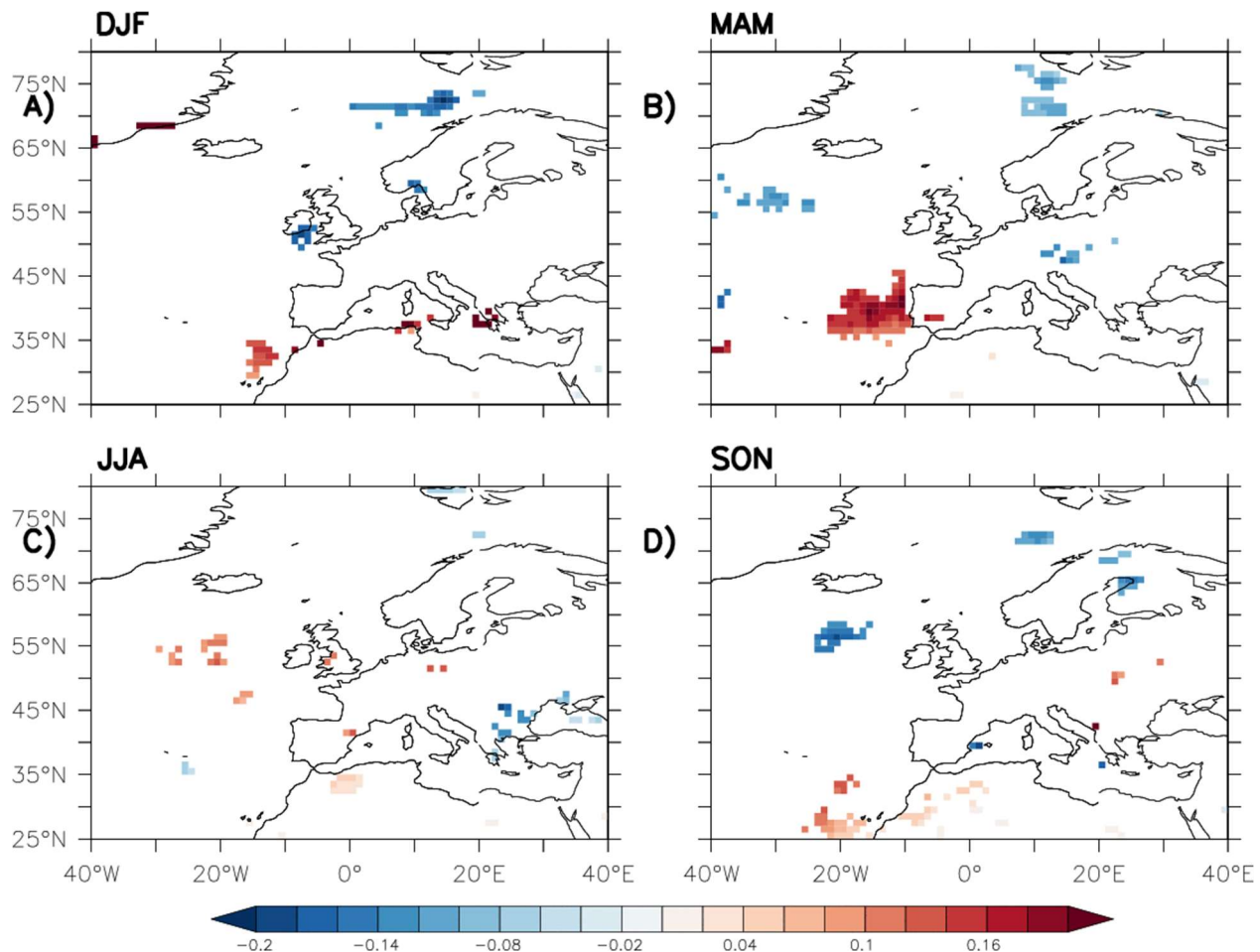


Figure 10: The impact of resolution on the precipitation response to the AMV. Units: mm./day.

Examination of the quadratures for mean sea-level pressure (psl) and surface air temperature (tas) reveals that there are no significant differences between the response to AMV between the resolutions. To illuminate this point further **Figure 11** shows the fraction of the total variance in spring (MAM) surface air temperature explained by each term in the ANOVA expression above. It is clear that there are significant differences in the mean climate (averaged across experiments) between resolutions, most notably over regions of high topography, but also over the oceans. There are also significant, if smaller differences between the responses to the phases of the AMV (**Figure 11b**). The impact of resolution and experiment combined is shown in **Figure 11c**, whilst there are regions where resolution appears to alter the modelled response to the AMV, these represent very small fractions of the variance that are not statistically significant. **Figure 11d** shows that the ensemble is dominated by the residual, or internal climate variability.

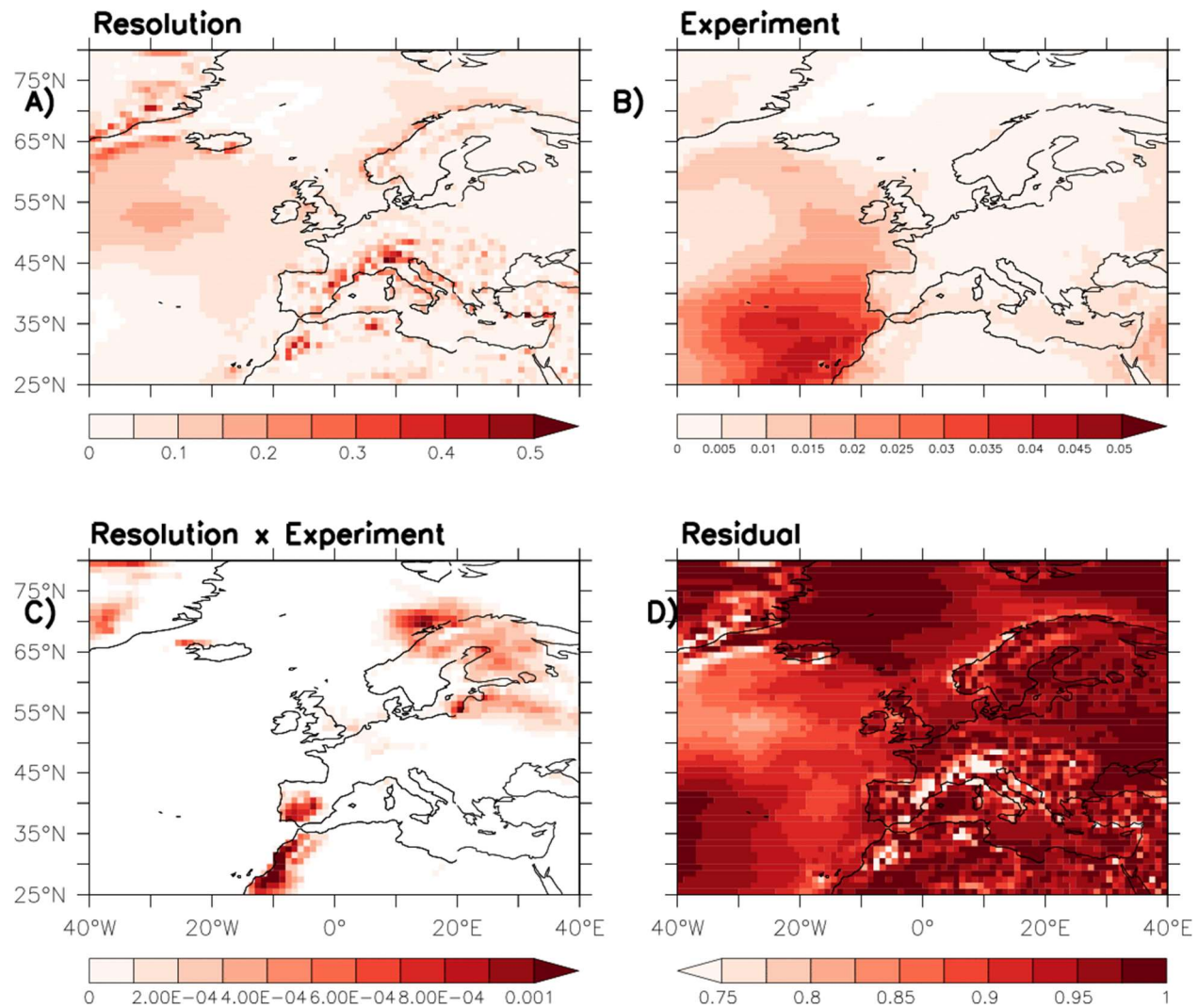


Figure 11: Fraction of the total variance in spring (MAM) surface air temperature explained by a) resolution (A) (H,L) b) experiment (B) (+,-) c) the interaction between the two (C), and a residual (E).

Key Points

In summary, there are notable and widespread modelled impacts of the AMV on European climate. These results are mainly consistent between the models used here, except perhaps for the atmospheric circulation response (psl) and surface air temperature over the Euro-Mediterranean region during summer and autumn. With this in mind, we now examine the response over this region in more detail.

3.4.3 The impact of Atlantic Multi-decadal variability on Euro-Mediterranean summer heat waves

We now focus on the specific regional impact of the AMV on Euro-Mediterranean summers.

Introduction

The links between the Atlantic Multi-decadal variability (AMV) and summer climate over the Euro-Mediterranean region have been documented in several studies using both models and observations. **Sutton and Hodson (2005)** showed that during a positive phase of the AMV, warmer conditions were obtained over central Europe, particularly over the Mediterranean basin. Concomitantly, a decrease in precipitation was obtained over this region while an increase was observed over the northern half of Europe (**Sutton and Dong 2012**). **Mariotti and Dell'Aquila (2011)** also found that about 30% of summer temperature anomalies over the Mediterranean basin are explained by the AMV. However, impacts of the AMV over the Euro-Mediterranean region have been documented in terms of mean climate, both in observations and models, but this is not the case for extreme events.

We now examine the impacts of the AMV over the Euro-Mediterranean region in terms of both mean climate and extreme events (heat waves) in summer in the AMV forcing experiments. For this analysis we focus on the LR configurations of CNRM-CM6 and EC-Earth3P. (This work will be extended to the remaining models in Table 2 at a later stage).

The AMV-forced response in this section is defined as the ensemble mean differences between the AMV+ and AMV- phases in the JJA (June-July-August).

AMV impact on Euro-Mediterranean climate

Consistent with previous studies based on observations (**O'Reilly et al 2017**), both models simulate a robust response in 2m temperature (T2m: tas) with a near surface warming of $\sim 0.6^{\circ}\text{C}$ over the Mediterranean basin in JJA, with positive AMV phase (**Figure 12**). Though less consistent than T2m response, the precipitation response (**Figure 13**) displays a dipole over the Europe-Mediterranean in both models, with negative (positive) anomalies South (North) of 45°N , with significant values over Scandinavia and the North Sea coasts, except for EC-Earth3P, in which, following the T2m response, drier conditions are also found over western Europe.

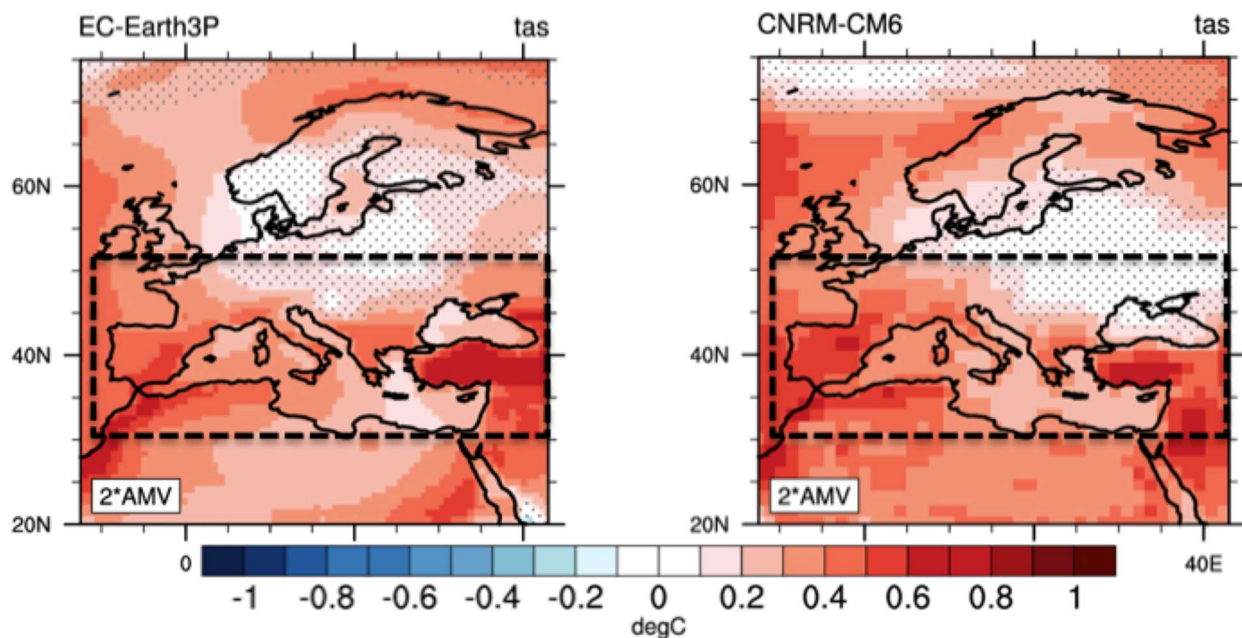


Figure 12: AMV-forced anomalies for June-August seasonal mean for T2m (shading interval is 0.1°C), for EC-Earth3P (left) and CNRM-CM6 (right). Stippling indicates regions that are below the 95% confidence level of statistical significance based on two-sided Student's t-test.

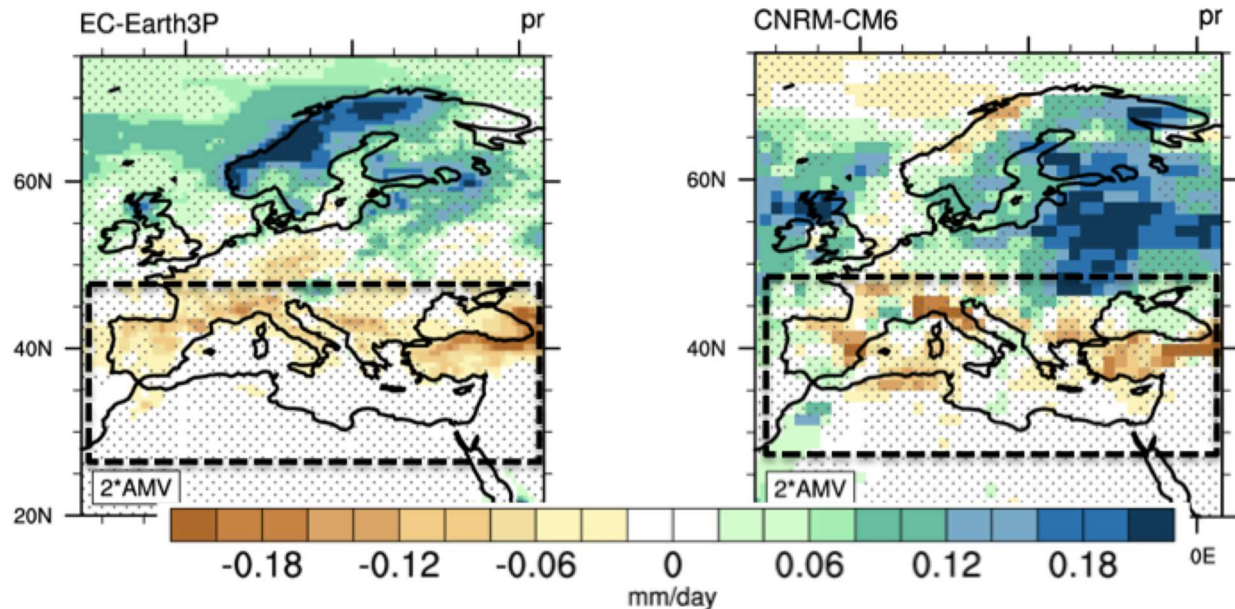


Figure 13: AMV-forced anomalies for June-August seasonal mean for precipitation, for EC-Earth3P (left) and CNRM-CM6 (right). Stippling indicates regions that are below the 95% confidence level of statistical significance based on two-sided Student's t-test

The atmospheric circulation response is also very robust for both models over the Mediterranean region, showing positive Z500 anomalies associated with anticyclonic conditions over this region (**Figure 14**), and also coherent with warmer and drier conditions shown in Figs. 1 and 2. However, regional differences can be found in Z500 responses over the Northern Europe.

We characterise the Heat Waves (HWs) following **Ruprich-Robert et al (2018)**. For a given amplitude of the AMV, and for each member of the AMV+ and AMV- ensemble, a HW is defined as a group of days that satisfy three criteria:

1. T_x must exceed T90 for at least three consecutive days
2. T_x averaged over the entire event must exceed T90
3. T_x for each day of the event must exceed the T75

where T_x is the daily maximum 2-m air temperature, and T90 (T75) corresponds to the 90th (70th) percentile of the T_x distribution built from all the members of the AMV+ and AMV- experiments during the June-July-August (JJA) period. The number of HW days corresponds to the number of days during summer that meet the HW criteria.

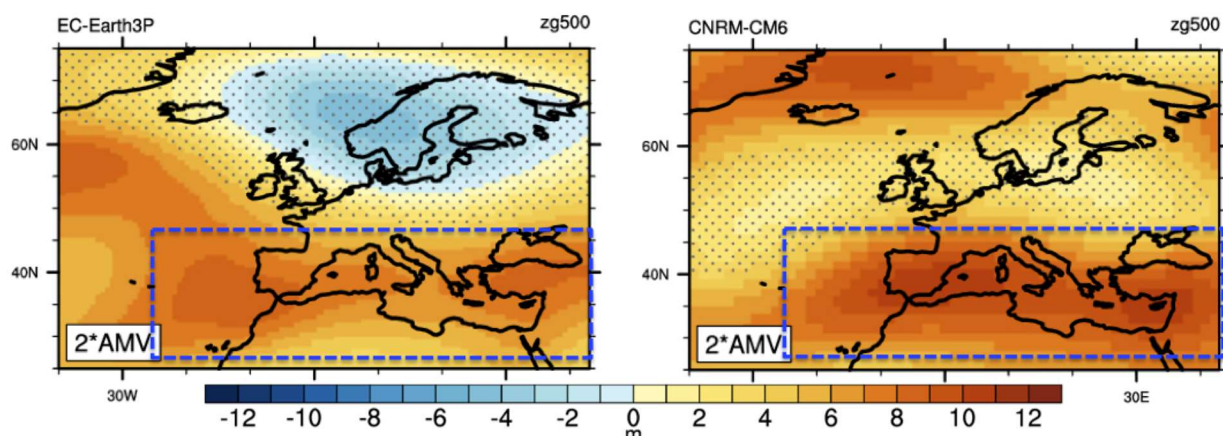


Figure 14: AMV-forced anomalies for June-August seasonal mean for Z500, for EC-Earth3P (left) and CNRM-CM6 (right). Stippling indicates regions that are below the 95% confidence level of statistical significance based on two-sided Student's t-test.

An increase in the number of HW days is obtained in both models over the Mediterranean basin (Figure 15). However, the location of the maximum anomalies differs between the two models: Anatolia, the Levant and Maghreb for EC-Earth3P, while Spain, Greece, Italy and Turkey are more impacted in CNRM-CM6. For both models, the number of HW days per summer over these regions is increased by ~20% on average (up to 50% over the eastern Mediterranean) relative to the climatological number of HW.

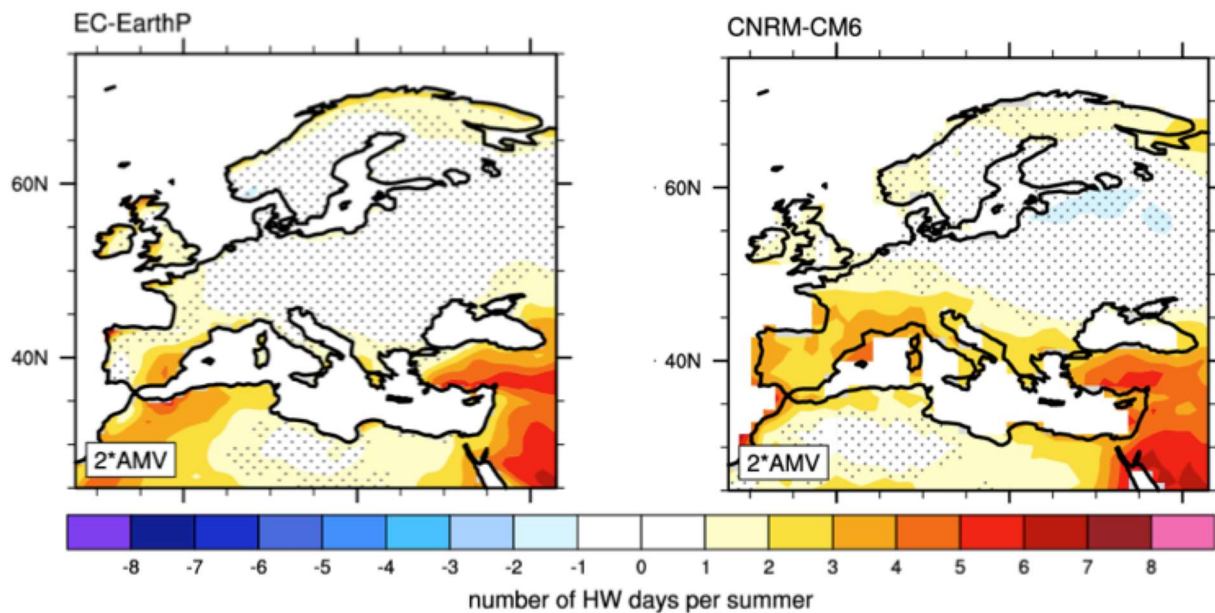


Figure 15: AMV-forced anomalies for June-August seasonal mean for number of heatwave days, for EC-Earth3P (left) and CNRM-CM6 (right). Stippling indicates regions that are below the 95% confidence level of statistical significance based on two-sided Student's t-test.

Mechanisms

We investigate the surface heat budget by looking at the surface downward net Shortwave (SW) and Longwave (LW) radiation fluxes, together with the surface downward net sensible (SH) and latent (LH) heat fluxes and their response to AMV. Here we adopt the same heat flux direction as in **Ruprich-Robert et al. 2018** in which a positive heat flux anomaly leads to a surface warming.

SW anomalies (Figure 16) are coherent with the climate response shown in **Figures 12-15** with positive SW around the Mediterranean basin (stronger SW response in CNRM-CM6 in the eastern Mediterranean). The lower troposphere associated with positive AMV and moistening associated with positive AMV also impact downward LW radiation. Over the eastern Mediterranean, both models show a reduction in latent heat loss (i.e. decrease in evapotranspiration), with stronger response in EC-Earth3P. These LH anomalies are also coherent with less precipitation and soil moisture decrease (not shown) displayed by both models. In summary, SW and LH seem to be the most important heat fluxes explaining the local thermodynamical response over the Mediterranean area, with stronger SW response in CNRM-CM6, and stronger LH response in EC-Earth3P.

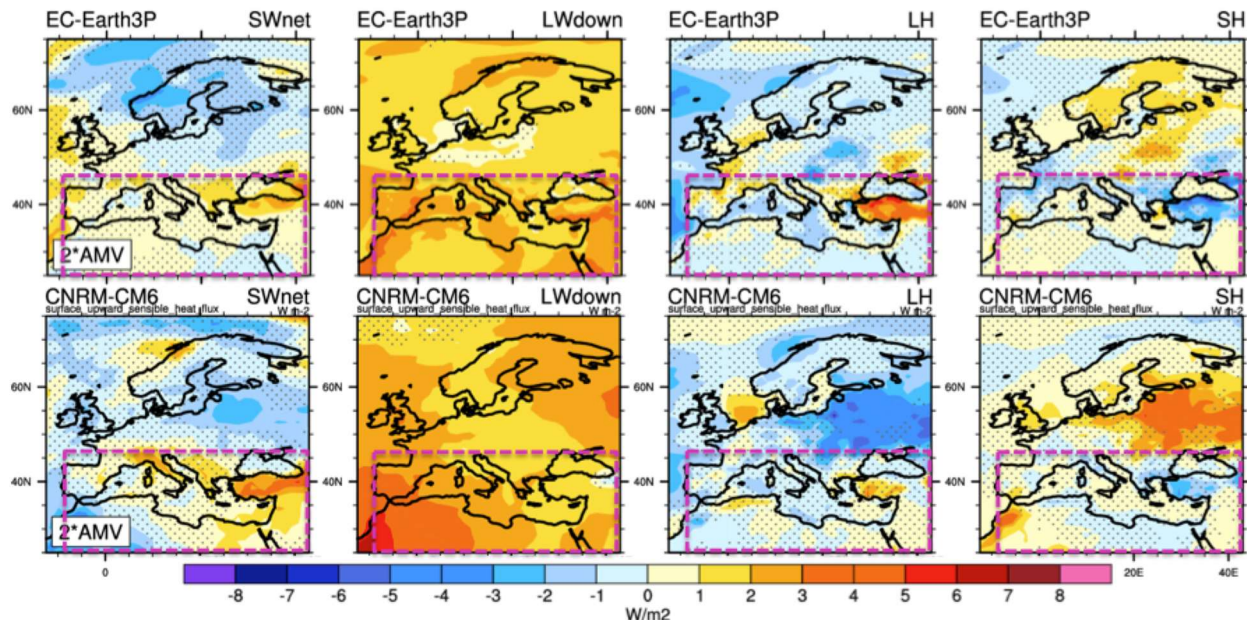


Figure 16: AMV-forced anomalies for June-August seasonal mean for SW, LWdown, LH and SH for EC-Earth3P (up) and CNRM-CM6 (bottom). Stippling indicates regions that are below the 95% confidence level of statistical significance based on two-sided Student's t-test.

In terms of mechanisms we focus here over the Mediterranean basin since it is the region where both models exhibit the most robust response. Several mechanisms to explain the AMV impact over the Mediterranean have been proposed in the past. They are based on both the tropical and extra-tropical AMV-forced SST anomalies. Here we investigate the role of the Tropical Atlantic: warmer conditions over the Tropical Atlantic (i.e. AMV+) can enhance the West African Monsoon (WAM) (**Zhang and Delworth 2006, Martin et al 2014**), which is also the case in our experiments (not shown). **Gaetani et al. (2011), Cassou et al (2005)**, among others, suggest that enhanced WAM can affect the direct meridional overturning circulation between the tropics and the Mediterranean basin. A stronger WAM can enhance the local Hadley cell and to increase both upper motions over the monsoon area and subsidence over the Mediterranean, leading to warmer and drier than normal conditions and increase of HW occurrence. **Figure 17** shows these mechanisms for CNRM-CM6: the warming induced by AMV+ (versus AMV-) can be seen in upper levels in the atmosphere. This leads to an increase in specific humidity around 15-25N over the monsoon area). The local hadley cell (middle) is enhanced with increased subsidence around 40N (Mediterranean area)

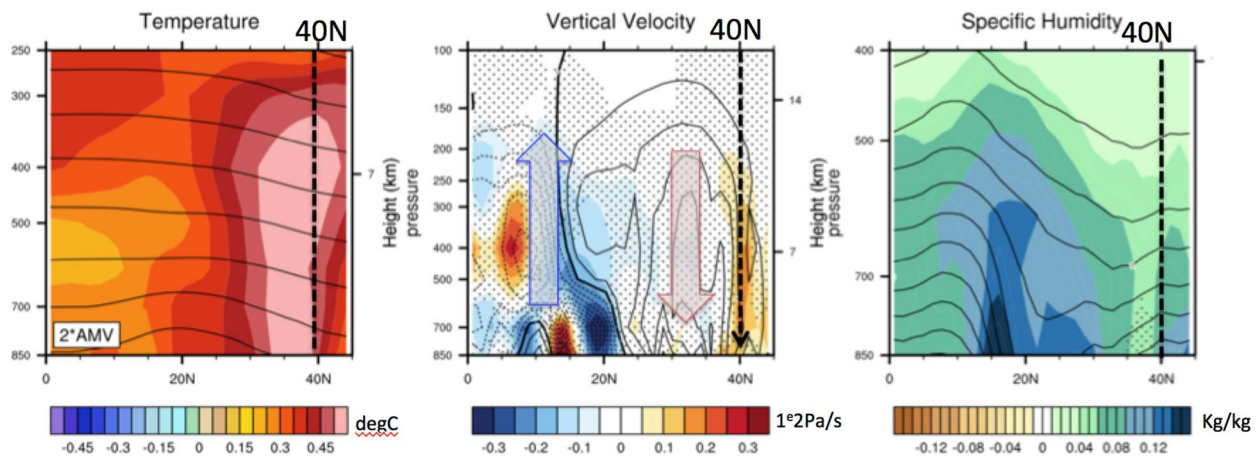


Figure 17: AMV-forced zonal response or June-August seasonal mean for temperature, vertical velocity and specific humidity averaged over 0-45N, 0-40E. Stippling indicates regions that are below the 95% confidence level of statistical significance based on two-sided Student's t-test.

These results have been submitted for publication (Qasmi et al. submitted) and we plan to extend this study to other models in Table 2.

Key Points

The AMV drives increased warmer and drier conditions over the Euro Mediterranean region during summer, leading to an increased number of heat-wave days in July and August. Analysis suggest this arises due to increased subsidence over the region, driven by AMV-induced changes to the West African Monsoon system.

3.4.4 Pacific Response to the AMV

We now extend our view to examine the global impacts of the AMV. In this section we focus on the specific remote impacts of the AMV on the Pacific region.

Introduction

We examine the AMV impacts in terms of 2-meter air temperature (T2m) and geopotential height 500hPa (ZG500) during the boreal winter season defined here as December to March (DJFM). In addition, we only discuss the difference between the 10-year ensemble mean average of the AMV+ and AMV- experiments.

Pacific Ocean response

In response to an observed AMV warming, models tend to simulate a tropical Pacific cooling that extends to the North Pacific through the East (Figure 1YRR). This cooling contrasts with warm anomalies over the Pacific NorthWest. The amplitude of those anomalies is model dependent. In particular, there is a factor 10 in the amplitude of the NINO3.4 SST index cooling between the response simulated by MPI-ESM1-2-HR and CNRM-CM6-LR. The reasons behind the AMV-tropical Pacific teleconnection and its inter-model spread are the subject of an article in preparation (**Ruprich-Robert et al.** in prep.).

The mechanism proposed is that warmer tropical Atlantic initiates changes in the Atlantic-Pacific Walker circulation in boreal summer, which modifies the western tropical Pacific surface winds. The Indo-Pacific Walker circulation accelerates in response to this surface wind changes. It acts as a positive feedback on the initial tropical Pacific response to the Atlantic forcing.

In summary, the Walker circulation changes eventually leads to the development of a tropical Pacific cooling in boreal winter (**Figure 18-left**). We found that the inter-model spread is mostly coming from the Indo-Pacific Walker circulation feedback and the strength of the associated atmospheric convection over the Warm Pool (**Figure 19-middle**). The latter is tightly linked to the Warm Pool warming response relatively to the upper tropospheric temperature of the whole tropical belt, which its inter-model spread appears to be controlled by the cooling response in the South Atlantic. Therefore, we conclude that, un-intuitively, the La Niña-like response to an AMV warming is ultimately constrained by the strength of the intertropical Atlantic surface temperature gradient (**Figure 19-right**). Finally, we tracked back the origin of the inter-model spread of this intertropical Atlantic temperature gradient and we found that it is coming from the different representation of SST-low cloud relationship among the models. The models simulating the strongest relationship are the models simulating the strongest La Niña-like anomalies in response to an AMV warming.

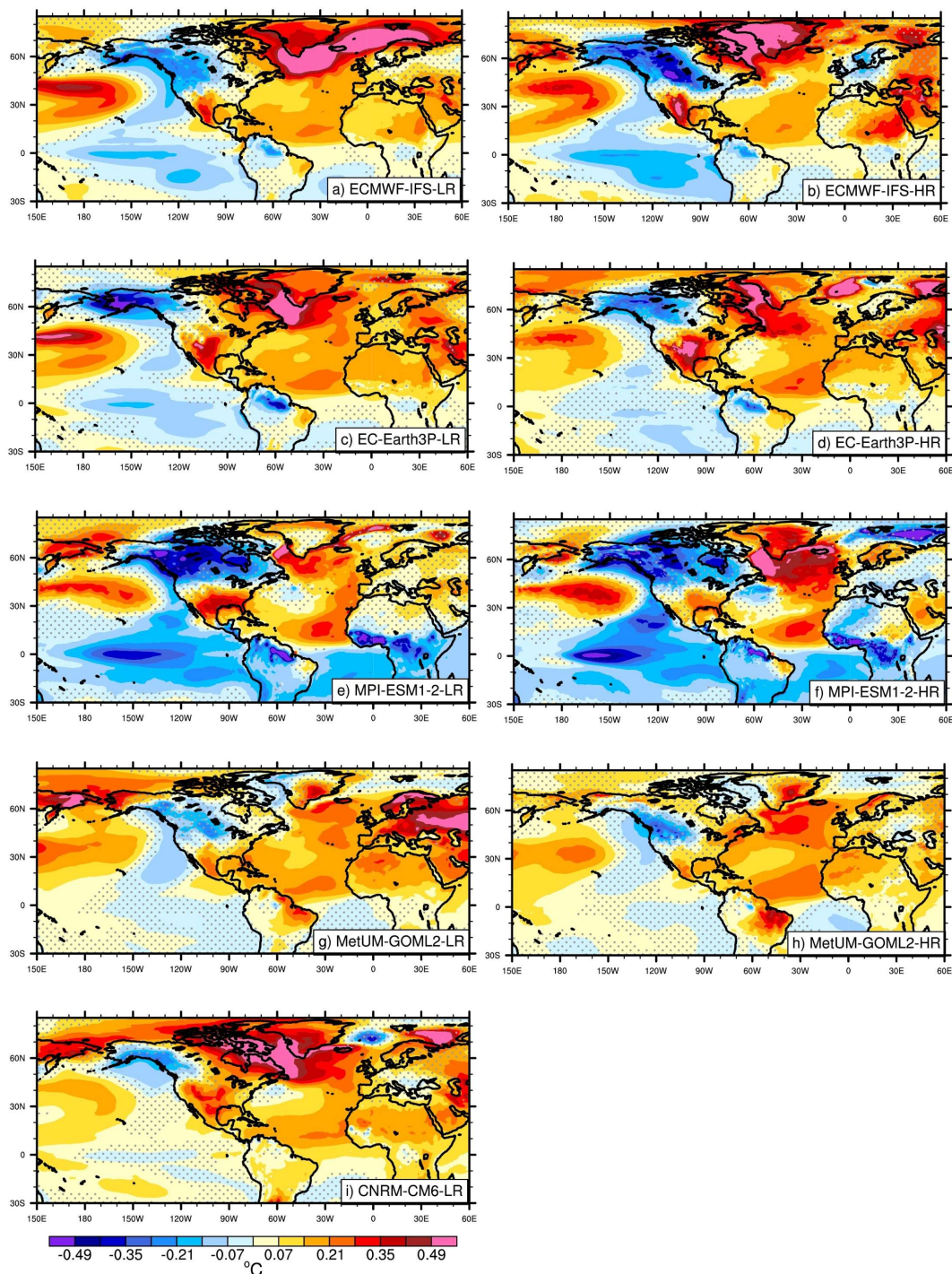


Figure 18: December-January-February-March 2-meter air temperature difference between the 10-year ensemble mean average of the AMV+ and AMV- experiments. Stippling indicates regions that are below the 95% confidence level of statistical significance according to a two-sided t-test.

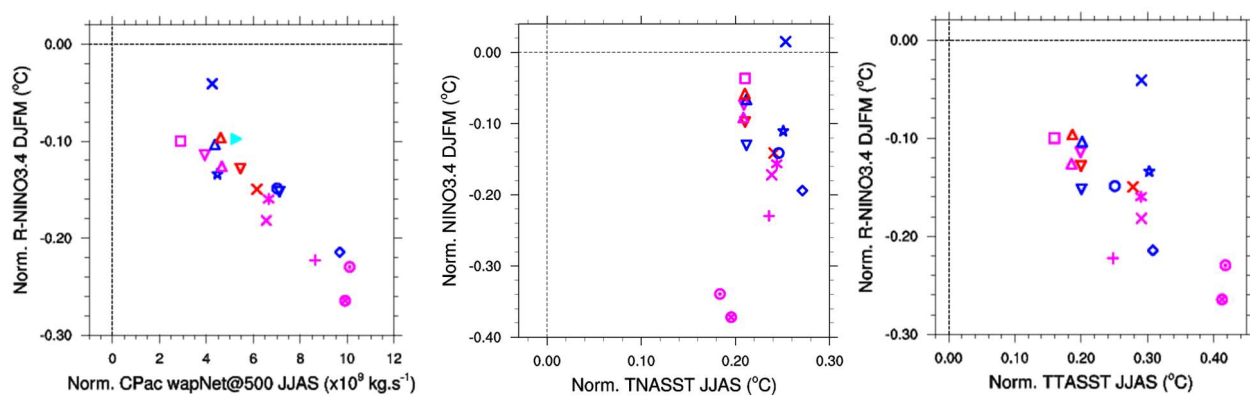


Figure 19: (left) Inter-model relationship between boreal winter NINO3.4 SST index and the boreal summer tropical North Atlantic SST. Each marker represents the ensemble mean 10-year averaged difference between AMV+ and AMV- simulations and each colour codes for different AMV forcing strength: 1xAMV, 2xAMV and 3xAMV strength in blue, magenta and red, respectively (simulation anomalies have been normalized by their respective AMV forcing strength). (middle) same as (left) but for the relative NINO3.4 SST index and the boreal summer central tropical Pacific net vertical mass transport at 500hPa. The relative NINO3.4 index is defined as the NINO3.4 SST index minus the tropical 20°S-20°N SST mean. Upward vertical mass transport is defined as negative by convention. (right) same as (middle) but between the relative NINO3.4 SST index and the boreal summer intertropical Atlantic SST gradient. On the (middle) and (right) panels, the percentage of covariance explained between the two variables are 81% and 45%, respectively. All the magenta markers represent results from the Primavera WP5 simulations except the triangles facing up and down.

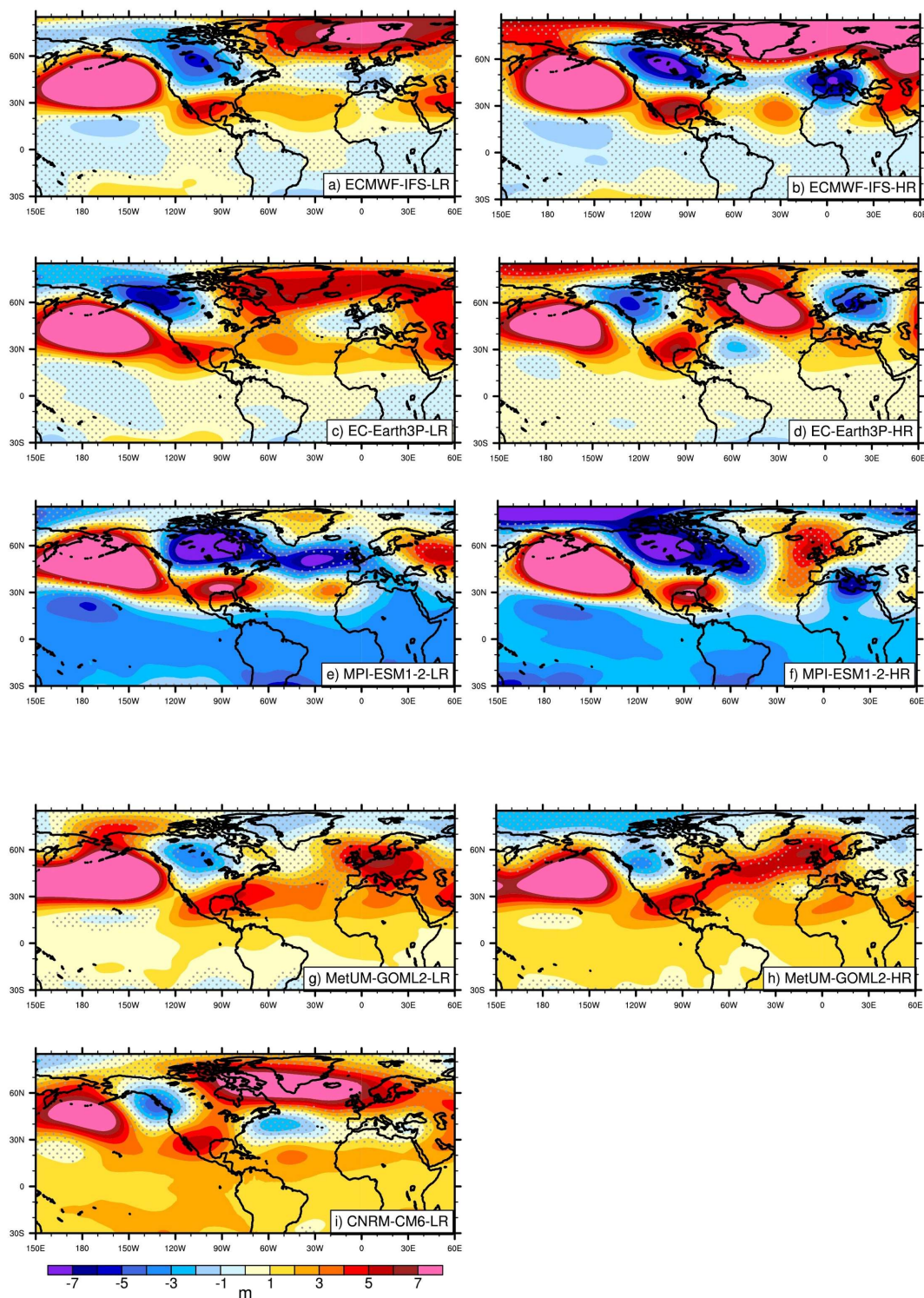


Figure 20 As Figure 18 but for 500 hPa Geopotential height (ZG500).

Continental response

In addition to the Pacific response, models simulate a warming over the south of North America and a cooling over the north-west of North America (**Figure 20**). Yet, the amplitude of the exact extension of this cooling is model dependent. For the 2 MPI-ESM1-2 models, the cooling extends over the entire Canada whereas for the EC-Earth3P-LR model the cooling is mostly confined to Alaska. Over the northern part of Africa, all the models except the 2 MPI-ESM1-2 models simulate a warming response to the AMV.

Over the Pacific-North America sector, all models simulate a Pacific North America (PNA) pattern response in its negative phase, with a decrease of the Aleutian low. Yet, the exact locations of the centres of action of the PNA response vary among models. This may also explain the difference between modelled temperature anomalies over North America. In particular, the models simulating cyclonic anomalies over the whole Canada also simulate cold anomalies all over Canada (e.g., MPI and ECMWF models).

There is a large inter-model spread response over Europe, especially over the north-west where some models simulate a cooling and other simulate a warming. A large inter-model spread is also found in the Z500 response to AMV over the North Atlantic - Europe region (**Figure 20**). The different atmospheric response among the models could therefore explain the differences in T2m response as argued in **Qasmi et al. (2020)**.

In particular, in the absence of atmospheric circulation response to an AMV warming, one would expect the presence of positive T2m anomalies over western Europe through the advection by the mean flow of warm anomalies from the North Atlantic. Following this perspective, the cyclonic anomalies over Europe simulated in the ECMWF-IFS-HR and MPI-ESM1-2-HR models could explain the absence of positive anomalies over western Europe. The study of the inter-model spread response to a warming in terms of North Atlantic - Europe atmospheric circulation is the object of a submitted article led by **Ruggieri et al. (submitted)**. In this study, we argue that in response to an AMV warming, the Atlantic storm track is contracted and less extended poleward and the low-level jet is shifted towards the equator in the Eastern Atlantic. We demonstrate a link between model bias and features of the jet response.

Key Points

The AMV drives remote climate impacts across the globe, in particular driving changes in the Pacific Ocean SST (tropical cooling). The AMV also drives widespread temperature changes across the North American Continent.

3.4.5 Global Monsoon response to AMV

We now focus on the specific remote impacts of the AMV on the Global Monsoon System. These results are discussed in more detail in **Monerie et al 2019**.

Introduction

The Global monsoon precipitation affects a significant fraction of the global population. Understanding what drives year-to-year changes in precipitation rates in these regions would aid in efforts to better predict and plan for such variations. Several studies have suggested that the AMV could modulate the global monsoon system (**Ting et al., 2011; Trenberth and Shea, 2006**). Here we examine the impact of the AMV on the global monsoon system in the AMV experiment ensemble. The analysis currently examines the impact on one of the models in **Table 2** (MetUM-GOML LR). Future analysis will extend this to all models.

Impact on the Global Monsoon system

The observed relationship between global precipitation and the AMV (**Figure 21a**) suggests that the AMV is associated with notable changes in tropical precipitation over the major monsoon systems across the globe. To deduce what aspects of these variations are due to the AMV we turn to the AMV experiments.

The impact of the AMV on global monsoon hemispheric summer precipitation is shown in **Figure 21b**. The AMV drives a northward shift in the Atlantic Inter-Tropical Convergence Zone (ITCZ), leading to increases in precipitation north of the equator, and a reduction to the south.

Notable changes are also driven outside the Atlantic basin - the West Pacific warm pool, the northern Indian Ocean, and North East India all see higher precipitation driven by the AMV.

Conversely, there are notable reductions over Brazil and Northern Australia.

Figure 21c shows these changes as region means, highlighting the significance of the precipitation over the SAM, AUS, NAF, and SAS monsoon regions. However, precipitation changes are not significant for NAM, SAF, and EAS, and for GM due to opposing responses between the Northern and the Southern Hemispheres. Some of these changes are consistent with the observed relationship (**Figure 21a**), which suggest change in the AMV may be the main driver of the observed changes in these regions. Other regions are not consistent with the observed relationship., which suggests that other external processes may have been responsible for the observed variation there.

There are also notable changes in the extent of regions affected by monsoon precipitation (**Figure 21d**). The AMV drives reductions in SAM, and AUS monsoon regions and increases in others (SAS, NAF, and EAS).

In summary, The AMV drives widespread global changes in the global monsoon system, which modifies not only precipitation rates, but also the spatial extent of global monsoon systems.

Key Points

The AMV drives widespread changes in the Global Monsoon system, leading to latitudinal shifts resulting in some regions receiving less monsoon rains, and some regions more.

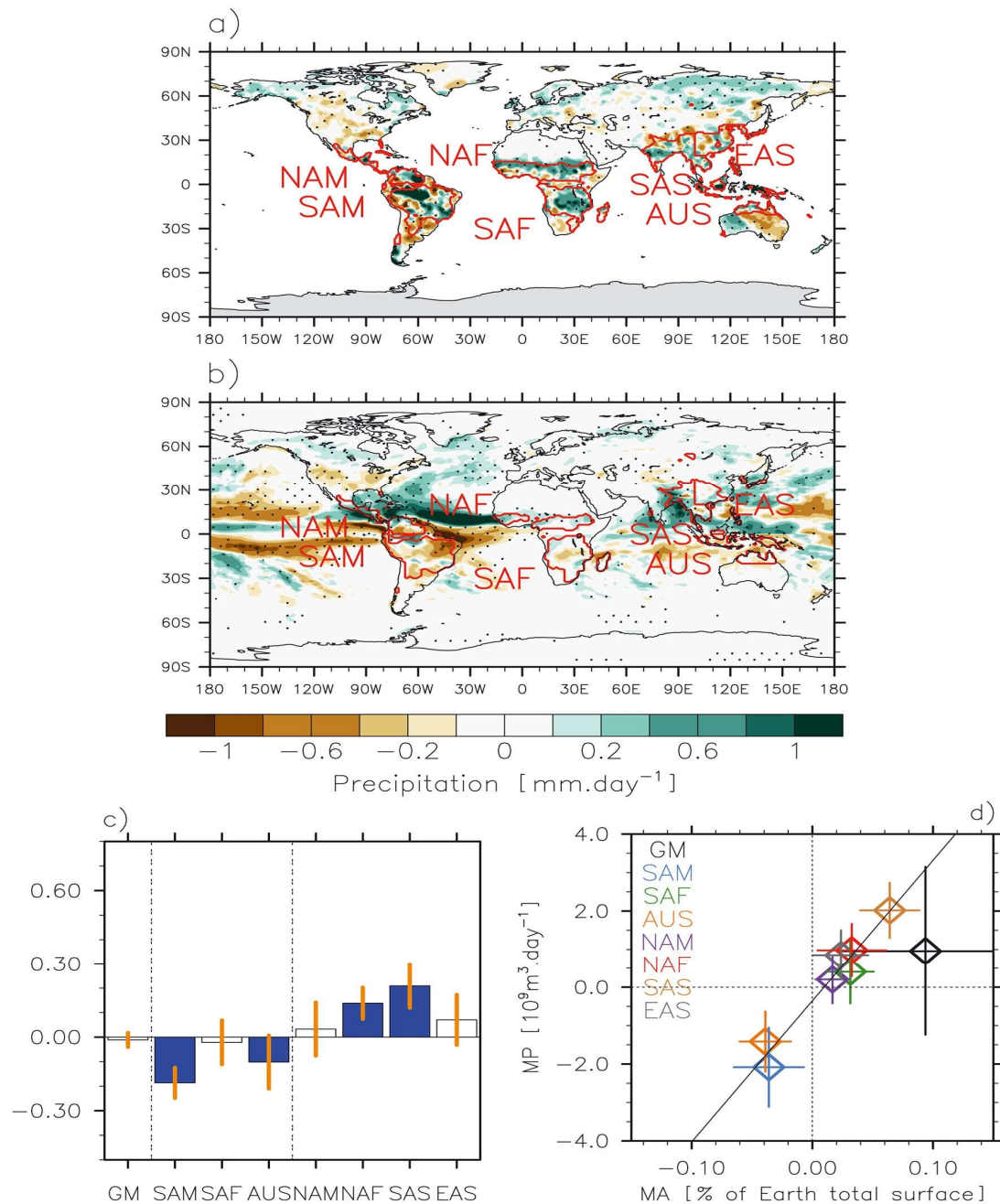


Figure 21: (a) Observed precipitation (mm/day; GPCC; Schneider et al., 2014) regressed onto the AMV index (ERSST; Huang et al., 2016). (b) Change in precipitation (mm/day) related to AMV (AMV+ minus AMV-). Monsoon domains are drawn in red. Precipitation anomalies are shown for MJJAS (NDJFM) for the Northern (Southern) Hemisphere. Stippling indicates that anomalies are significantly different to zero according to a Student's t test at the 95% confidence level. (c) Changes in monsoon index (MI; mm/day) for AMV+ minus AMV-. A blue bar indicates significant changes according to a Student's t test at the 95% confidence level. Orange vertical lines show two standard errors. (d) Change in monsoon area (MA; percent of the Earth total surface) versus the change in monsoon precipitation (MP; total area weighted precipitation, in 10⁹ m³/day). Vertical and horizontal coloured lines indicate two standard errors for both MP and MA. The black line is the MA—MP linear regression (excluding GM). For (c) monsoon domains are not fixed and computed separately from each member and experiment. NAM = North America; SAM = South America; SAF = southern Africa; NAF = North Africa; SAS = South Asia; AUS = Australia; EAS East Asia; AMV = Atlantic multidecadal variability; ERSST = extended

reconstructed sea surface temperature; MJJAS = May to September; NDJFM = November to March; GM = global monsoon. Reproduced from **Monerie et al 2019**

3.5 Conclusions

We have presented the results of the WP5 AMV multi-model multi-resolution experimental ensemble. These experiments demonstrate that the AMV drives significant climatic impacts over Europe, these include warmer surface air temperatures over large parts of Europe, changes in atmospheric circulation patterns (pls) across all seasons, and significant changes in precipitation, particularly over western coastal regions, but also in the Euro-Mediterranean region. These different models used in this study generally agree on these impacts, although there are some regions where the model disagree - notably regions to the north of Scandinavia and the Euro-Mediterranean region. We have examined the summer drying in this latter region in some detail and will extend this analysis to the full model ensemble in a future analysis.

We have assessed how increasing model resolution affects the climate impacts of the AMV. In most cases, despite model resolution significantly affecting model climatology, it does not generally affect the overall impact of the AMV over Europe in the climate variables we have examined here. One notable exception is over small regions of high European topography in spring and summer rainfall, where resolutions does make small, but significant differences in the AMV response. Resolution is still likely to play a role in some climatic processes that we have not analysed here, e.g. hurricanes. Future research will examine the role of resolution in the AMV response.

Further afield, we have examined the influence of the AMV on the Pacific Ocean, North America and the global monsoon system. We have demonstrated that the AMV drives significant impacts across the globe. Future studies will extend this analysis to examine the impact of model choice and resolution on the global impacts of the AMV.

Further analysis of the AMV across the PRIMAVERA models (including the historical simulation ensemble) can be found in the companion WP2 deliverable: D2.4 *Assessment of the impact of large-scale drivers (from WP5) on processes that benefit from increased resolution across the multi-model ensemble, and their sensitivity to climate change based on the WP6 Stream 1 simulations.*

Assessment for the future

The ultimate driver of the AMV is still a matter of scientific debate, but we have demonstrated here that future changes in the AMV could have notable impacts on climate over the European region and further field. Such changes may increase or decrease the impact of the long-term global warming trend, depending on the future phase of the AMV. Uncertainties remain in the response in some regions - most notably the impact in summer over the Euro-Mediterranean region. Further research

will focus on understanding the origin of these modelling uncertainties. For the climate variables we have examined here (temperature, precipitation and mean sea-level pressure), increasing model resolution does not generally alter the modelled response of the AMV over Europe.

3.6 References

G.Balsamo, P.Viterbo, A.Beljaars, B.van den Hurk, M.Hirschi, A.K.Betts, K.Scipal, 2009, A revised hydrology for the ECMWF model, *J. Hydro.Met.*, <https://doi.org/10.1175/2008JHM1068.1>.

Boer G J, Smith D M, Cassou C, Doblas-Reyes F, Danabasoglu G, Kirtman B, Kushnir Y, Kimoto M, Meehl G A, Msadek R, Mueller W A, Taylor K E, Zwiers F, Rixen M, Ruprich-Robert Y and Eade R 2016 The Decadal Climate Prediction Project (DCPP) contribution to CMIP6 *Geosci. Model Dev.* **9** 3751–77

Booth, B. B. B., N. J. Dunstone, P. R. Halloran, T. Andrews, and N. Bellouin, 2012: Aerosols implicated as a prime driver of twentieth-century North Atlantic climate variability. *Nature*, **484**, 228–232, <https://doi.org/10.1038/nature10946>.

Bouillon, S., Maqueda, M. A. M., Legat, V., and Fichefet, T.: Anelastic–viscous–plastic sea ice model formulated on Arakawa Band C grids, *Ocean Modell.*, 27, 174–184, 2009

Cassou C, Terray L and Phillips A S 2005 Tropical Atlantic Influence on European Heat Waves *J. Climate* **18** 2805–11

Craig, A., Valcke, S., & Coquart, L. (2017). Development and performance of a new version of the OASIS coupler, OASIS3-MCT_3.0.

Geoscientific Model Development Discussion, 10, 3297–3308. <https://doi.org/10.5194/gmd-2017-64>

Decharme, B., Delire, C., Minvielle, M., Colin, J., Vergnes, J. P., Alias, A., et al. (2019). Recent changes in the ISBA-CTRP land surface

system for use in the CNRM-CM6 climate model and in global off-line hydrological applications. *Journal of Advances in Modeling Earth Systems*, 11. <https://doi.org/10.1029/2018MS001545>

Déqué, M., Dreveton, C., Braun, A., & Cariolle, D. (1994). The ARPEGE/IFS atmosphere model: A contribution to the French community climate modelling. *Climate Dynamics*, 10(4-5), 249–266. <https://doi.org/10.1007/BF00208992>

Dong, B., and A. Dai, 2015: The influence of the interdecadal Pacific oscillation on temperature and precipitation over the globe. *Climate Dyn.*, **45**, 2667–2681, <https://doi.org/10.1007/s00382-015-2500-x>.

Enfield, D. B., A. M. Mestas-Nuñez, and P. J. Trimble, 2001: The Atlantic multidecadal oscillation and its relation to rainfall and river flows in the continental U.S. *Geophys. Res. Lett.*, **28**, 2077, doi:<https://doi.org/10.1029/2000GL012745>.

Fichefet, T. and Maqueda, M.: Sensitivity of a global sea ice model to the treatment of ice thermodynamics and dynamics, *J. Geo-phys. Res.-Oceans*, 102, 12609–12646, 1997

Gaetani M, Pohl B, Douville H and Fontaine B 2011 West African Monsoon influence on the summer Euro-Atlantic circulation *Geophys. Res. Lett.* **38**

Gent, P.R. and J.C. Mcwilliams, 1990: [Isopycnal Mixing in Ocean Circulation Models](#). *J. Phys. Oceanogr.*, **20**, 150–155, [https://doi.org/10.1175/1520-0485\(1990\)020<0150:IMOCM>2.0.CO;2](https://doi.org/10.1175/1520-0485(1990)020<0150:IMOCM>2.0.CO;2)

Hazeleger, W., Bintanja, R. Studies with the EC-Earth seamless earth system prediction model. *Clim Dyn* **39**, 2609–2610 (2012). <https://doi.org/10.1007/s00382-012-1577-8>

Hirons, L. C., Klingaman, N. P., and Woolnough, S. J.: MetUM-GOML1: a near-globally coupled atmosphere–ocean-mixed-layer model, *Geosci. Model Dev.*, **8**, 363–379, <https://doi.org/10.5194/gmd-8-363-2015>, 2015.

Henley, B. J., J. Gergis, D. J. Karoly, S. B. Power, J. Kennedy, and C. K. Folland, 2015: A tripole index for the interdecadal Pacific oscillation. *Climate Dyn.*, **45**, 3077–3090, <https://doi.org/10.1007/s00382-015-2525-1>.

Huang, B., P.W. Thorne, T. M. Smith, W. Liu, J. Lawrimore, V. F. Banzon, H--M. Zhang, T. C. Peterson and M. Menne, 2016: Further Exploring and Quantifying Uncertainties for Extended Reconstructed Sea Surface Temperature (ERSST) Version 4(v4), 2016. *J. Climate*, **29**, 3119--3142, doi: <https://doi.org/10.1175/JCLI-D-15-0430.1>

Jungclaus, J. H., Fischer, N., Haak, H., Lohmann, K., Marotzke, J., Matei, D., Mikolajewicz, U., Notz, D., and von Storch, J. S. (2013), Characteristics of the ocean simulations in MPIOM, the ocean component of the MPI-Earth system model, *J. Adv. Model. Earth Syst.*, **5**, 422– 446, doi:[10.1002/jame.20023](https://doi.org/10.1002/jame.20023).

Kerr, R. A., 2000: A North Atlantic climate pacemaker for the centuries. *Science*, **288**, 1984–1985, <https://doi.org/10.1126/science.288.5473.1984>.

Kirchner-Bossi, N., García-Herrera, R., Prieto, L. and Trigo, R.M. (2015), A long-term perspective of wind power output variability. *Int. J. Climatol*, **35**: 2635-2646. doi:[10.1002/joc.4161](https://doi.org/10.1002/joc.4161)

Knight, J. R., R. J. Allan, C. K. Folland, M. Vellinga, and M. E. Mann, 2005: A signature of persistent natural thermohaline circulation cycles in observed climate. *Geophys. Res. Lett.*, **32**, L20708, <https://doi.org/10.1029/2005GL024233>.

Madec G, Bourdallé-Badie R, Bouttier P-A, Clément Bricaud, Diego Bruciaferri, Daley Calvert, et al. (2017). NEMO ocean engine. <https://doi.org/10.5281/ZENODO.1472492>

Mariotti A and Dell'Aquila A 2012 Decadal climate variability in the Mediterranean region: roles of large-scale forcings and regional processes *Clim Dyn* **38** 1129–45

Martin E R and Thorncroft C D 2014 The impact of the AMO on the West African monsoon annual cycle: Impact of AMO on West African Monsoon *Q.J.R. Meteorol. Soc.* **140** 31–46

Masson, V., Le Moigne, P., Martin, E., et al. (2013). The SURFEXv7.2 land and ocean surface platform for coupled or offline simulation of earth surface variables and fluxes. *Geoscientific Model Development*, **6**(4), 929–960. <https://doi.org/10.5194/gmd-6-929-2013>

McCabe, G., Palecki, M.A , Betancourt J (2004), Pacific and Atlantic Ocean influences on multidecadal drought frequency in the United States *PNAS*, **101** (12) 4136-4141; DOI: [10.1073/pnas.0306738101](https://doi.org/10.1073/pnas.0306738101)

Monerie, P.-A., Robson, J., Dong, B., Hodson, D. L. R., & Klingaman, N. P. (2019). Effect of the Atlantic multidecadal variability on the global monsoon. *Geophysical Research Letters*, 46, 1765–1775. <https://doi.org/10.1029/2018GL080903>

Noilhan, J., & Planton, S. (1989). A simple parameterization of land surface processes for meteorological models. *Monthly Weather Review*,

117(3), 536–549. [https://doi.org/10.1175/1520-0493\(1989\)117<0536:ASPOLS>2.0.CO;2](https://doi.org/10.1175/1520-0493(1989)117<0536:ASPOLS>2.0.CO;2)

O'Reilly C H, Woollings T and Zanna L 2017 The Dynamical Influence of the Atlantic Multidecadal Oscillation on Continental Climate *J. Climate* **30** 7213–30

Otterå, O. H., M. Bentsen, H. Drange, and L. L. Suo, 2010: External forcing as a metronome for Atlantic multidecadal variability. *Nat. Geosci.*, **3**, 688–694, <https://doi.org/10.1038/ngeo955>.

Qasmi S., Sanchez-Gomez E., Ruprich-Robert Y., Boe J., Cassou C : Modulation of the occurrence of heat waves over the Euro-mediterranean region by the intensity of the Atlantic Multidecadal Variability, submitted.

Roberts, C. D., Senan, R., Molteni, F., Boussetta, S., Mayer, M., and Keeley, S. P. E.: Climate model configurations of the ECMWF Integrated Forecasting System (ECMWF-IFS cycle 43r1) for HighResMIP, *Geosci. Model Dev.*, 11, 3681–3712, <https://doi.org/10.5194/gmd-11-3681-2018>, 2018.

Ruprich-Robert, Y., R. Msadek, F. Castruccio, S. Yeager, T. Delworth, and G. Danabasoglu, 2017: [Assessing the Climate Impacts of the Observed Atlantic Multidecadal Variability Using the GFDL CM2.1 and NCAR CESM1 Global Coupled Models](#). *J. Climate*, **30**, 2785–2810, <https://doi.org/10.1175/JCLI-D-16-0127.1>

Ruprich-Robert Y, Delworth T, Msadek R, Castruccio F, Yeager S and Danabasoglu G 2018 Impacts of the Atlantic Multidecadal Variability on North American Summer Climate and Heat Waves *J. Climate* **31** 3679–700

Salas Mélia, D. (2002). A global coupled sea ice–ocean model. *Ocean Modelling*, 4(2), 137–172. [https://doi.org/10.1016/S1463-5003\(01\)00015-4](https://doi.org/10.1016/S1463-5003(01)00015-4)

Schneider, U., Becker, A., Finger, P. et al. GPCC's new land surface precipitation climatology based on quality-controlled in situ data and its role in quantifying the global water cycle. *Theor Appl Climatol* **115**, 15–40 (2014). <https://doi.org/10.1007/s00704-013-0860-x>

Smith, D. M., and Murphy, J. M. (2007), An objective ocean temperature and salinity analysis using covariances from a global climate model, *J. Geophys. Res.*, 112, C02022, doi:[10.1029/2005JC003172](https://doi.org/10.1029/2005JC003172).

Stevens, B, M. Giorgetta, M. Esch, T. Mauritsen, T. Crueger, S. Rast, M. Salzmann, H. Schmidt, J. Bader, K. Block, R. Brokopf, I. Fast, S. Kinne, L. Kornblueh, U. Lohmann, R. Pincus, T. Reichler, and E. Roeckner. Atmospheric component of the mpi-m earth system model: Echam6. *Journal of Advances in Modeling Earth Systems*, 5:146-172, 2013. doi:[10.1002/jame.20015](https://doi.org/10.1002/jame.20015)

Sutton R T and Hodson D L R 2005 Atlantic Ocean Forcing of North American and European Summer Climate *Science* **309** 115–8

Sutton R T and Dong B 2012 Atlantic Ocean influence on a shift in European climate in the 1990s *Nature Geosci* **5** 788–92

Ting, M., Kushnir, Y., Seager, R., & Li, C. (2011). Robust features of Atlantic multi-decadal variability and its climate impacts. *Geophysical Research Letters*, 38, L17705. <https://doi.org/10.1029/2011GL048712>

Trenberth, K. E., & Shea, D. J. (2006). Atlantic hurricanes and natural variability in 2005. *Geophysical Research Letters*, 33, L12704. <https://doi.org/10.1029/2006GL026894>

Valcke, S.: The OASIS3 coupler: a European climate modelling community software, *Geosci. Model Dev.*, 6, 373–388, <https://doi.org/10.5194/gmd-6-373-2013>, 2013.

Vancopenelle M (2012) http://www.climate.be/users/lecomte/LIM3_users_guide_2012.pdf

Voldoire, A., Saint-Martin, D., Sénési, S., Decharme, B., Alias, A., Chevallier, M., et al. (2019). Evaluation of CMIP6 DECK experiments with CNRM-CM6-1. *Journal of Advances in Modeling Earth Systems*, 11, 2177– 2213. <https://doi.org/10.1029/2019MS001683>

Walters, D., Boutle, I., Brooks, M., Melvin, T., Stratton, R., Vosper, S., Wells, H., Williams, K., Wood, N., Allen, T., Bushell, A., Copsey, D., Earnshaw, P., Edwards, J., Gross, M., Hardiman, S., Harris, C., Heming, J., Klingaman, N., Levine, R., Manners, J., Martin, G., Milton, S., Mittermaier, M., Morcrette, C., Riddick, T., Roberts, M., Sanchez, C., Selwood, P., Stirling, A., Smith, C., Suri, D., Tennant, W., Vidale, P. L., Wilkinson, J., Willett, M., Woolnough, S., and Xavier, P.: The Met Office Unified Model Global Atmosphere 6.0/6.1 and JULES Global Land 6.0/6.1 configurations, *Geosci. Model Dev.*, 10, 1487–1520, <https://doi.org/10.5194/gmd-10-1487-2017>, 2017.

Zhang R and Delworth T L 2006 Impact of Atlantic multidecadal oscillations on India/Sahel rainfall and Atlantic hurricanes *Geophysical Research Letters* 33 Online: <https://agupubs.onlinelibrary.wiley.com/doi/abs/10.1029/2006GL026267>

3.7 Peer Review articles

Monerie, P.-A., Robson, J., Dong, B., Hodson, D. L. R., & Klingaman, N. P. (2019). Effect of the Atlantic multidecadal variability on the global monsoon. *Geophysical Research Letters*, 46, 1765–1775. <https://doi.org/10.1029/2018GL080903>

3.8 Planned future Publications

Qasmi S., Sanchez-Gomez E., Ruprich-Robert Y., Boe J., Cassou C : Modulation of the occurrence of heat waves over the Euro-Mediterranean region by the intensity of the Atlantic Multidecadal Variability, *submitted*.

Ruggieri et al. Impact of model uncertainty on European circulation response to the AMV (*submitted*).

Ruprich-Robert et al. AMV-Pacific teleconnections in the AMV experiments(*in prep.*)

Overview paper for the PRIMAVERA WP5 ensemble experiments detailing the global response to the AMV and the impact of model choice and resolution. *Submit in 2020*

4. Lessons Learnt

The key scientific and technical lessons learnt by the WP5 project team from the experiments in T5.1 are:

Scientific

1. The AMV drives widespread climate impacts in climate models.
2. These impacts are relatively insensitive to the choice of climate model used to assess these impacts, or the spatial resolution of that model.
3. There are widespread remote ocean responses to the AMV that could not be seen by the previous generation of atmosphere-only forced AMV experiments.

Technical

1. There are large challenges involved in performing large-ensemble experiments with high resolution climate models.
2. Converting climate model data output to a commonly agreed standard to allow coherent analysis between models still presents a significant challenge to the climate modelling community.
3. Storage and analysis of this data presents a significant challenge, joint large-scale data analysis IT infrastructure is essential in this regard

5. Links Built

The results from the WP5 AMV experiments have directly contributed to WP2's analysis of large-scale drivers of climate (D2.4: *Assessment of the impact of large-scale drivers (from WP5) on processes that benefit from increased resolution across the multi-model ensemble, and their sensitivity to climate change based on the WP6 Stream 1 simulations.*)

The results are being used in wider multi-model assessments of the impact of the AMV, both inside and outside the central CMIP6 DCPP-C AMV analysis project.